# Electrified Natural Gas Pyrolysis to Produce Low-Carbon Hydrogen

**Navid Teymouri**

**A Thesis**

**in**

**The Department**

**of**

**Chemical and Materials Engineering**

**Presented in Partial Fulfillment of the Requirements**

**for the Degree of**

**Master of Applied Science (Chemical and Materials Engineering) at**

**Concordia University**

**Montréal, Québec, Canada**

**August 2023**

CONCORDIA UNIVERSITY

School of Graduate Studies

This is to certify that the thesis prepared

By: **Navid Teymouri**

Entitled: **Electrified Natural Gas Pyrolysis to Produce Low-Carbon Hydrogen**

and submitted in partial fulfillment of the requirements for the degree of

**Master of Applied Science (Chemical and Materials Engineering)**

complies with the regulations of this University and meets the accepted standards with respect to originality and quality.

Signed by the Final Examining Committee:

_____ Chair
*Dr. Melanie Hazlett*

_____ Examiner
*Dr. Ivan Kantor*

_____ Examiner
*Dr.*

_____ Supervisor
*Dr. Yaser Khojasteh-Salkuyeh*

Approved by _____
Sana Jahanshahi Anbuhi, Graduate Program Director
Department of Chemical and Materials Engineering

_____ 2023

_____
Mourad Debbabi, Dean
Faculty of Engineering and Computer Science

# Abstract

Electrified Natural Gas Pyrolysis to Produce Low-Carbon Hydrogen

Navid Teymouri

Electrified plasma-assisted natural gas pyrolysis (PNGP) emerges as a promising technology for low-carbon hydrogen production in this thesis, encompassing process simulation, economic evaluation, and environmental impact assessment. The technical analysis demonstrates an impressive carbon yield of approximately 95% from natural gas, showcasing highly efficient decomposition to carbon particles and hydrogen. However, PNGP requires a specific energy of 16.2 $kWh/kgH_2$, which surpasses conventional steam methane reforming (SMR). Economic evaluations reveal the hydrogen minimum selling price for PNGP to be $4.5 per kilogram. The inclusion of revenues from carbon black production, priced at $\$0.4/kg$, reduces PNGP's minimum selling price by $\$1/kgH_2$, enhancing its competitiveness with SMR. Environmental assessments underscore PNGP's potential for mitigating greenhouse gas (GHG) emissions when integrated with renewable electricity sources. Comparisons with SMR and PEM electrolysis emphasize the importance of carbon black production credits in bolstering PNGP's economic and environmental performance. Furthermore, a comparison of the cost of avoided/captured greenhouse gas (GHG) emissions between PNGP and SMR with CCS shows that PNGP offers competitive advantages, particularly when the carbon black production credits are considered in the system. At certain electricity and natural gas price levels, PNGP's cost of avoided/captured emissions becomes more favorable compared to SMR with CCS. This finding highlights the potential of PNGP as a promising option for low-emission hydrogen production, considering both its technical performance and environmental sustainability.

# Acknowledgments

Throughout the course of this thesis, I have been fortunate to receive an exceptional amount of support and assistance from various individuals and institutions. Foremost, I extend my immense gratitude to my supervisor, Professor Yaser Khojasteh-Salkuyeh, whose unwavering support and invaluable guidance illuminated my path. His insightful feedback and encouragement propelled me to refine my ideas and elevate the quality of my work.

I am also deeply appreciative of Marzieh Shokrollahi, Philippe Navarri, and my friends in CSTAR for their remarkable collaboration, empathy, and unwavering support, which fostered a conducive research environment.

Furthermore, I wish to express my heartfelt thanks to my wife, Azadeh, for her selfless support and companionship throughout this journey. Her encouragement and belief in me have been a constant source of strength.

Lastly, I am sincerely grateful to Concordia University and its staff for providing exceptional facilities, organizing enriching events, and offering impactful classes, all of which have played a pivotal role in shaping my academic journey. Their contributions have been invaluable in the successful completion of this thesis.

# Contents

# List of Figures

# List of Tables

# Nomenclature

| | |
|---|---|
| $(g)$ | Gas Phase |
| $(s)$ | Solid Phase |
| $AF$ | Annualization Factor |
| $CEPCI$ | Chemical Engineering Plant Cost Index |
| $E_T$ | Total Energy Demand $(MW)$ |
| $eff$ | Efficiency |
| $i$ | Interest Rate |
| $k_i$ | Reaction Rate Constant |
| $LHV$ | Lower Heating Value $(MJ/kg)$ |
| $m$ | Mass Flow $(kg/h)$ |
| $N$ | Number of Years |
| $n$ | Cost Scaling Factor |
| $R$ | Universal Gas Constant |
| $T$ | Temperature |
| APEA | Aspen Process Economic Analyser |
| CB | Carbon Black |

CCS Carbon Capture and Storage

DC Direct Current

ENGP Electrified Natural Gas Pyrolysis

FCI Fixed Capital Investment

GHG Greenhouse Gases

IRR Internal Rate of Return

MMUSD Million US Dollars

NG Natural Gas

PEME Proton Exchange Membrane Electrolysis

PNGP Plasma-assisted Natural Gas Pyrolysis

PSA Pressure Swing Adsorption

SER Specific Energy Requirement

SMR Steam Methane Reforming

TCI Total Capital Investment

TRL Technology Readiness Level

w With

w/o Without

# Chapter 1

# Introduction

## 1.1 Background and Motivation

Hydrogen is an essential component in achieving the global net-zero goals. It is considered a clean energy source for transportation and heavy industries and can be used as a feedstock for chemical production and carbon capture and utilization technologies. However, the production of low-emission hydrogen with competitive economic performance is a significant challenge.

Currently, hydrogen production primarily comes from fossil fuels, with natural gas accounting for 48%, oil for 30%, and coal for 18% [1]. It is accountable for more than 900 million tonnes of annual $CO_2$ emissions [2] where steam methane reforming (SMR) as the most common industrial method of hydrogen production has the overall GHG emissions of around 11.9 $kgCO_2eq/kgH_2$[3]. At the same time, global hydrogen consumption was reported to exceed 94 million tonnes in 2021 where the main consumers were petroleum refineries and chemical production facilities [2]. It is expected to reach 530 million tonnes by 2050 where it will mostly be consumed in transportation and chemical and steel production industries [4].

Although water electrolysis is envisaged as the main source of hydrogen production in 2050's net-zero emission scenario, it is presently an energy-intensive method with electricity consumption of more than 50 $kWh/kgH_2$ [5]. Furthermore, while electrolyzers are not direct fossil fuel consumers, this method of hydrogen production cannot be considered to be totally green since up to 70% of global electricity generation is currently based on fossil fuels [6]. The emergence of the

environmental situations thus seems to be in need of some short-term solutions to help us with this matter by acting as a bridge passing through the status quo towards the net-zero goals.

One solution to address the challenge of producing low-carbon hydrogen would be electrified natural gas pyrolysis (ENGP) through which natural gas, which is mainly methane, is decomposed into hydrogen and carbon. Unlike SMR, this method has no direct GHG emissions but has the potential to produce carbon black as a valuable by-product [7]. Being an endothermic reaction (74.5 $kJ/molCH_4$) [8], methane decomposition needs an energy input to proceed. Conventional pyrolysis uses fossil fuels to provide the heat required for the process while in the electrified process, the required energy can be provided by electricity. Nevertheless, it is anticipated that the electrified pyrolysis process would exhibit lower sensitivity towards electricity consumption rates compared to present-day electrolysis methods, underscoring its potential as a feasible short-term alternative for low-carbon hydrogen production.

## 1.2 Research Objective

The objective of this study is to analyze the electrified natural gas pyrolysis (ENGP) process using plasma heating technology. A comprehensive process simulation of the technology will be conducted using Aspen Plus® software. The kinetic modeling of methane decomposition and heat integration of the process will be conducted in detail. The outcome of the process simulation will be utilized to estimate the specific energy requirements of the process in terms of hydrogen production capacity.

The economic evaluation of the ENGP process and its comparison with other hydrogen production methods, including SMR and water electrolysis, is a crucial aspect of this study, aimed at identifying the optimal strategy with minimal financial gaps and GHG reduction costs. The minimum selling price of hydrogen produced from the ENGP process will be estimated and analyzed in the context of various parameters, such as natural gas and electricity prices, primary equipment costs, and the market price of carbon black. By comparing these prices with those of other hydrogen production methods, the competitiveness of the ENGP process will be evaluated.

The subsequent stage of this study involves the environmental impact assessment of the ENGP

process, including all upstream activities/processes. The assessment will determine the overall greenhouse gas (GHG) emissions as well as other critical impacts of the process. The assessment will also consider the potential impact of carbon black production as a by-product of the process, to determine if the system can positively contribute to reducing the impact of global warming by avoiding additional product generation. To further evaluate the potential of electrified natural gas pyrolysis as a short-term solution for low-carbon hydrogen production, this study will conduct case studies comparing the GHG emissions of different electricity sources as well as the impact of the geographical location of the system. These case studies will analyze the results of the impact assessment in order to determine the viability of ENGP as a solution. Specifically, these results will provide valuable insight into the impact of ENGP on GHG emissions and will assist in determining whether the 2030 Emissions Reduction Plan targets of reducing emissions levels to 40% below 2005 levels can be achieved in Canada [9].

## 1.3 Thesis Layout

Chapter 2 of this thesis presents a comprehensive review of the current methods and applications of hydrogen production, including emerging technologies and future estimations. In chapter 3, the assumptions, design data, and other relevant details of the plasma-assisted natural gas pyrolysis (PNGP) process simulation will be discussed and a simulation case will be developed to determine the process efficiency, energy consumption, and other requirements. subsequently, this chapter will focus on the environmental impact assessment and economic evaluation of the PNGP process based on the technical results obtained from process simulation. In chapter 4, the performance of the PNGP process will be evaluated against other hydrogen production technologies in terms of various aspects. Finally, chapter 5 provides conclusions and answers to the research questions and objectives of this study.

# Chapter 2

# Literature Review

Chapter 2 of this thesis presents a comprehensive literature review on hydrogen production methods, focusing on both established techniques and emerging technologies. The chapter begins by providing an overview of the current landscape of hydrogen production, highlighting the dominant methods such as steam methane reforming and water electrolysis. The literature review explores the principles, advantages, and limitations of these conventional approaches, along with their associated energy requirements and environmental impacts. Furthermore, the chapter delves into the emerging technology of methane decomposition, which offers a promising alternative for hydrogen production. The review covers recent advancements in methane decomposition techniques, including plasma-assisted and catalytic processes, and evaluates their feasibility, efficiency, and potential for scalability. By critically examining the literature, this chapter aims to provide a comprehensive understanding of the current state-of-the-art in hydrogen production methods, laying the groundwork for the subsequent chapters' analysis and evaluation.

## 2.1 Hydrogen Background

Hydrogen serves as a versatile energy carrier with a diverse array of applications. It finds utility as an important feedstock in industries such as steel production, chemical manufacturing, and petroleum refining, while also exhibiting potential for employment in transportation, heating systems, and power generation. Global hydrogen demand was reported to reach 94 million tonnes in

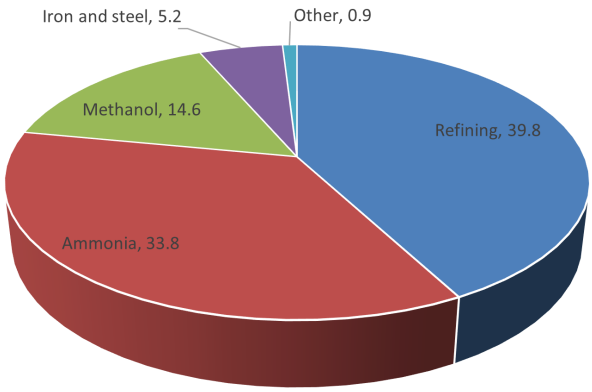


Figure 2.1: 2021 global hydrogen demand by sector (million tonnes) [2]

2021 (Figure 2.1) [2]. The broad spectrum of hydrogen's applications underscores its significance in the pursuit of current decarbonization objectives. However, the prevalent method of hydrogen production involves reforming fossil fuels [2], a process that is inherently linked to significant emissions released into the atmosphere, thus conflicting with the sustainability goals mentioned above. Nonetheless, the growing demand for hydrogen necessitates exploring and advancing novel technologies capable of generating hydrogen with minimal carbon footprints.

Methane decomposition, also referred to as pyrolysis, presents a promising avenue for hydrogen production with reduced $CO_2$ emissions by converting methane or other hydrocarbons into hydrogen and carbon under oxygen-free conditions. Over the past three decades, extensive research has been conducted to explore diverse techniques within this domain, focusing on catalyst enhancement, reactor design, catalyst deactivation, and regeneration mechanisms, as well as process electrification employing various mediums. This chapter critically examines these prior investigations, preceded by a concise introduction to some prevalent hydrogen production approaches.

## 2.2 Hydrogen Production

There are two primary methods employed for hydrogen production: fossil fuels reforming (i.e., steam reforming, partial oxidation, and auto thermal reforming), which relies on non-renewable sources, and water electrolysis using renewable electricity. The former approach can be augmented

with carbon capture and storage (CCS) technologies to mitigate the overall greenhouse gas emissions associated with the process. Conversely, the latter approach is regarded as fully aligned with carbon net zero objectives, as it relies on renewable energy and contributes much less to carbon emissions [10].

### 2.2.1 Hydrogen from Fossil Fuels

Among the fossil fuels reforming techniques, steam methane reforming (SMR) holds a prominent position, significantly contributing to the current hydrogen market. SMR involves the reaction between natural gas, predominantly methane, and high-temperature steam, resulting in the production of hydrogen, carbon monoxide, and carbon dioxide when it is coupled with a water-gas shift reaction. the process can be represented by the following equations[11]:

$$CH_4(g) + H_2O(g) \rightarrow CO(g) + 3H_2(g); \Delta H_{298K} = 206kJ/mol \tag{1}$$

$$CO(g) + H_2O(g) \rightarrow CO_2(g) + H_2(g); \Delta H_{298K} = -41kJ/mol \tag{2}$$

This process enjoys widespread adoption due to its cost-effectiveness and the abundant availability of methane feedstock. Nevertheless, SMR operations are accompanied by carbon dioxide emissions, which contribute to greenhouse gas emissions and the ongoing challenges of climate change.

Spath et al. [3] conducted an estimation of the life cycle greenhouse gas (GHG) emissions, reporting a value of 11.9 $kgCO_2eq/kgH_2$. Within this estimate, 75% of the emissions were attributed to the direct emissions resulting from the steam methane reforming (SMR) process. In a 2022 report by the International Renewable Energy Agency (IRENA) [10], a range of 9 to 11 $kgCO_2eq/kgH_2$ was presented as the emissions associated with SMR. These findings have stimulated significant research efforts toward improving the efficiency and environmental sustainability of SMR.

For instance, Salkuyeh et al. [12] reported a remarkable 70% reduction in SMR process emissions when integrating a carbon capture and storage (CCS) section, albeit with a 37% increase in natural gas consumption for the process. Notably, among the available options for $CO_2$ storage, geological storage has emerged as the most feasible approach. This involves injecting and storing $CO_2$ in geological formations, such as depleted oil and gas reservoirs [6]. However, the availability

of suitable geological formations for $CO_2$ storage may pose limitations and incur additional costs for $CO_2$ transportation.

### 2.2.2 Hydrogen from Water Electrolysis

Water electrolysis for hydrogen production is gaining attention due to its potential for achieving zero carbon emissions. This is primarily due to its ability to be powered by renewable energy sources like solar, wind, and hydropower. As a result, it has become an attractive option for clean and sustainable hydrogen production, aligning with the global decarbonization goals. Current estimates indicate that water electrolysis contributes to only 0.1% of global hydrogen production [13].

There are two primary types of water electrolysis: alkaline electrolysis and proton exchange membrane (PEM) electrolysis. The typical power consumption ranges from 50 to 60 kWh per kilogram of hydrogen produced [14]. However, it is important to note that if the electrolyzer is powered by non-renewable energy sources such as fossil fuels, significant carbon emissions are associated with the overall carbon footprint of hydrogen production.

Figure 2.2 illustrates the global electricity production shares in 2021 with renewable resources contributing only approximately 28% [15]. This, coupled with the energy intensity of current electrolyzers highlights the limitations of water electrolysis in hydrogen production. Researchers have conducted studies to assess the impact of electricity generation's carbon footprint on water electrolysis.

For instance, Lee et al. [16] investigated the potential $CO_2$ emissions of an alkaline water electrolysis process under various electricity production scenarios. They reported the $CO_2$ emissions of 30.7 $kgCO_2eq/kgH_2$ for the current Korean electricity mix, which predominantly relies on fossil fuels, compared to 3.1 $kgCO_2eq/kgH_2$ when electricity is derived entirely from renewable resources [16].

Another study by Palmer et al. [17] examined the life cycle greenhouse gas (GHG) emissions of a large-scale solar-powered alkaline electrolyzer. They reported GHG emissions of 4.3 $kgCO_2eq/kgH_2$ and 2.3 $kgCO_2eq/kgH_2$ for defined solar-grid and solar-battery scenarios, respectively. These studies show that hydrogen production through current water electrolysis technology is only environmentally favorable when combined with renewable electricity.

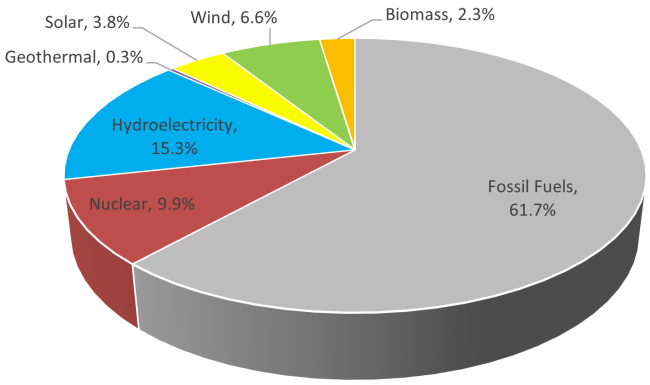


Figure 2.2: Global electricity production shares in 2021 taken from the US EIA [15]

## 2.3 Methane Pyrolysis

Methane decomposition, also known as methane pyrolysis, is a process that involves breaking down methane into hydrogen and solid carbon. The reaction occurs at high temperatures, typically above 1200 °C, and in an oxygen-free environment. The process can be represented by the following equation[8]:

$$CH_4(g) \rightarrow C(s) + 2H_2(g); \Delta H_{298K} = 74.5kJ/mol \tag{3}$$

The methane decomposition process has the advantage of not directly releasing carbon dioxide to the environment in comparison to steam methane reforming (SMR). However, it also presents specific challenges. One significant challenge is the requirement for high temperatures, which necessitates a significant amount of energy input. Achieving and maintaining these elevated temperatures can be energy-intensive and may counterbalance the environmental benefits associated with reduced carbon emissions. The use of catalysts in the process can potentially lower the operating temperature but introduces additional complexity. Consequently, extensive efforts have been devoted to optimizing the process and decreasing energy consumption through advancements in reactor design, catalyst development, and efficient heat transfer mechanisms.

### 2.3.1 Catalytic Methane Decomposition

As a result of the high stability of C-H bonds in methane, its thermal decomposition into hydrogen and carbon usually involves temperatures surpassing 1200 °C [18]. However, the use of catalysts can significantly lower the required temperature to a range of 500 to 900°C, depending on the specific catalyst employed [6]. Extensive research has been conducted on catalyst materials for methane decomposition, with two primary categories being identified: metal-based and carbon-based catalysts. Typically, metal catalysts exhibit superior initial activity and enable lower operating temperatures, but they tend to deactivate more quickly. On the other hand, carbon catalysts are more cost-effective and retain activity over a longer period, albeit at higher operating temperatures when compared to metal catalysts.

Transition metals, including nickel, iron, and cobalt, have been found to exhibit enhanced catalytic activity and suitability for methane decomposition. In their work, Li and Smith [19] compared Ni and Co catalysts for $CH_4$ decomposition and carbon removal with $O_2$. Ni catalyst showed higher activity and stability, while both catalysts underwent oxidation during regeneration. They noticed that oxygen reacted with carbon during $CH_4$ decomposition, yielding $CO$ and $CO_2$ impurities in the product.

Rahman et al. [20] investigated the catalytic decomposition of methane using Ni catalysts and determined that the optimal temperature range for the process was between 500 and 550°C. The amount of catalyst was found to have a significant influence on both the catalyst activity and deactivation, with smaller amounts leading to higher initial activity but faster deactivation. Catalyst regeneration was reported to be a challenge, as complete gasification of the carbon resulted in a significant loss of activity.

Jang and Cha [21] demonstrated the technical feasibility of $CO_2$-free hydrogen production through the catalytic decomposition of methane using $Fe/Al_2O_3$ catalyst. They investigated the impact of operational parameters on hydrogen yield in a fluidized bed reactor and found that increasing reactor temperature led to higher hydrogen yield while increasing superficial velocity resulted in decreased hydrogen yield.

Otsuka et al. [22] demonstrated the repeated production of hydrogen through catalytic methane

decomposition followed by the oxidation of carbon nanofibers employing Ni and Pd-Ni catalysts. Carbon fibers deposited on Ni catalysts were completely removed by oxidation at 753 K, while higher temperatures were required for complete carbon removal on Pd–Ni.

Activated carbons and carbon blacks with different textural properties and surface chemistry have been investigated as catalysts for methane decomposition. Although the activation energy of methane decomposition will reduce using these types of catalysts, it will still be higher compared to metal catalysts [23]. Carbon catalysts also tend to rapid deactivation during methane decomposition due to carbon deposition [24] and thus needed to be regenerated. To address the catalyst deactivation issue, Muradov et al. [25] conducted modeling and scaling-up studies of a fluidized bed reactor with carbon catalyst particles for the catalytic decomposition of natural gas as a solution to continuously operate the process. Their models accurately predicted methane conversion based on experimental data with carbon catalysts.

Table 2.1: Selected previous studies on catalyst deactivation/regeneration

| **Catalyst** | **regenerating Agent** | **Temperature** | **Regeneration Product(s)** | **Notes** | **Reference** |
|---|---|---|---|---|---|
| $Ni/SiO_2$ | Steam | $650°C$ | $H_2, CO_2, CO$ | - | [26] |
| $Ni/Al_2O_3$ | Oxygen | $500°C$ | $CO_2, CO$ | partial regeneration; full regeneration destroys catalyst activity | [20] |
| $Fe/Al_2O_3$ | - | $650°C$ | - | by attrition of carbon formed on catalyst surface | [21] |
| Activated Carbon | $CO_2$ | $1000°C$ | $CO$ | - | [27] |
| $Ni, Pd-Ni$ | $CO_2, O_2$ | $500°C$ | $CO$ | - | [21] |
| $Ni$ | $H_2$ | $500-600°C$ | $CH_4$ | selective carbon gasification with $H_2$ at the carbon-catalyst interface | [21] |

Table 2.1 provides a summary of some of the studies conducted on catalyst deactivation/regeneration of catalytic methane decomposition. Based on what has been reviewed, a major challenge in scaling up the technology to industrial levels is catalyst deactivation. Conventional regeneration methods using air and steam can lead to the production of carbon dioxide and carbon monoxide, thereby increasing process emissions and contaminating the hydrogen product while other proposed methods add up to the complexity of the process.

### 2.3.2 Thermal Plasma-assisted Pyrolysis

Various approaches have been proposed to supply the necessary energy for the thermal decomposition of methane, including solar energy, electric furnace, molten metal media, and plasma. Among these, plasma-assisted pyrolysis is of particular interest and will be discussed in this section as it has the highest technology readiness level (TRL) compared to other methods [28].

Plasma can be classified into two types: thermal and non-thermal, depending on whether the ionization process is predominantly influenced by gas temperature or electron energy, respectively [29]. Thermal plasma involves heating gas to several thousand degrees Celsius, resulting in the dissociation and ionization of gas molecules. This ionized gas, or plasma, comprises electrons, ions, and neutral particles, possessing unique characteristics such as high energy density and reactivity. On the other hand, non-thermal plasma refers to a partially ionized gas at or near room temperature. Unlike thermal plasma, it does not require high temperatures to maintain the plasma state. Instead, non-thermal plasma is generated by applying an electric field or other forms of energy to a gas, causing a fraction of the gas particles to become ionized while the overall gas remains at lower temperatures[29]. Studies have indicated that non-thermal plasma leads to lower methane conversions, whereas thermal plasma conversions exceed 80% [7].

Thermal plasma-assisted pyrolysis offers several advantages, including its catalyst-free nature and the ability to process various feedstocks encompassing a wide range of gaseous or liquid hydrocarbons [30]. The energy required for the process is supplied through an electrical discharge, typically facilitated by direct current (DC) plasma torches, arc plasma torches, or radio frequency induction plasma torches, which generate hot plasma gas. The selection of plasma gas can vary significantly, ranging from pure gases like nitrogen, helium, argon, oxygen, hydrogen, and gaseous hydrocarbons, to combinations thereof [30].

The application of this technology can be traced back to the 1990s when Kvaerner Engineering, in collaboration with SINTEF, pioneered its use for hydrogen and carbon black production from natural gas. They utilized a specially designed DC plasma torch that employed hydrogen as the plasma gas, achieving thermal efficiencies of 95-99% [31]. Although Kvaerner later established a commercial plant in Canada, technical difficulties led to its decommissioning within a few years

[32].

In a study by Fulcheri and Schwob [33] the energy requirement of methane decomposition to hydrogen and carbon black using plasma technology is estimated to be less than $2kWh/Nm^3H_2$ (i.e., $22kWh/kgH_2$). The technology was reported to offer high yields of carbon black production in comparison with the furnace black process as the most common method of carbon black production with much lower yields and higher $CO_2$ emissions.

Fincke et al. [34] developed a detailed kinetic model of methane pyrolysis and compared it with experimental results where they used a mixture of hydrogen and argon as plasma gas. they reported that The specific energy requirement (SER) for methane conversion is approximately $1.2kWh/Nm^3H_2$, which is about 30% higher than the minimum theoretical SER. The use of a separate plasma gas increases the requirement by 10%. Hence, efficient waste heat recovery and thermal management are crucial to approach the thermodynamic minimum SER.

In 2013, Monolith Materials, a US-based corporation, acquired the rights to Kvaerner Engineering's thermal plasma technology and established a pilot plant in California, followed by the construction of an industrial-scale plant in Nebraska [35].

It is claimed that the technology enables the simultaneous production of hydrogen and carbon black, with the ability to obtain different grades of carbon black by controlling the temperature and mixing conditions of feedstock and plasma gas [36]. A part of the hydrogen-rich gas produced, containing at least 60% hydrogen, is used in the process as plasma gas [37].

Based on the patents assigned to Monolith Materials Inc. [37, 38] the plasma reactor (Figure 2.3) consists of a plasma chamber and a reaction chamber, separated by a restriction area known as the throat, which prevents feedstock from entering the plasma generating zone, minimizing fouling and improving carbon black structure. Furthermore, the expansion from the restriction to the reaction area creates recirculation, preventing carbon black from adhering to the reactor walls and minimizing heat losses [38].

The plasma torch typically includes two concentric electrodes made of graphite, with the plasma gas flowing through the annulus between the electrodes [37]. Various gas flow paths can be used to enhance electrode cooling and heat transfer, such as splitting the gas flow to direct a portion through the annulus and the inner and outer spaces of the electrodes for shielding and wear reduction [37].

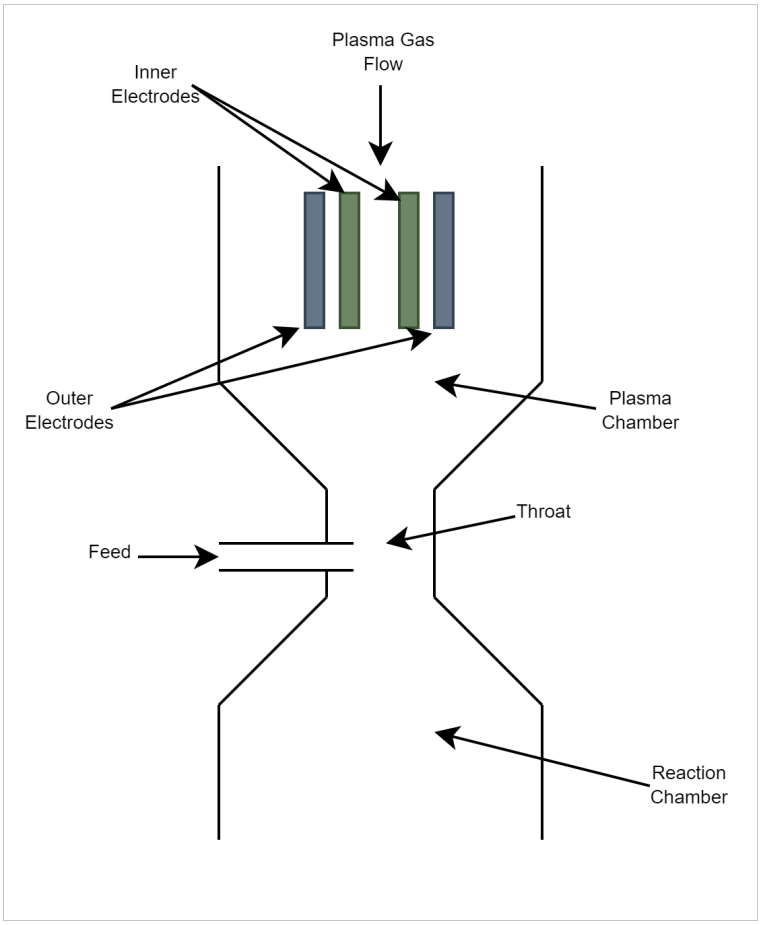


Figure 2.3: Plasma reactor scheme (Monolith Materials Inc.)[37, 38]

To enable the use of higher plasma temperatures, a regenerative cooling mechanism is employed, utilizing recycled plasma gas to cool the graphite liners of the plasma chamber, resulting in energy savings [39]. Additionally, an external heating setup has been introduced to heat the specific regions of the reactor walls, improving heat transfer and carbon black quality while reducing fouling [40].

Experimental results indicate a carbon yield of approximately 95% when using natural gas as the feedstock, indicating nearly complete decomposition to carbon particles and hydrogen [30], resulting in the production of high-quality carbon black as a valuable byproduct. The presence of this valuable byproduct is expected to positively impact the economic performance of the process. A visualization of the current global market share of carbon black, with the tire industry as the primary consumer, is presented in Figure 2.4. The carbon black market has witnessed substantial growth, with a reported global market volume of 14 million tonnes, which is projected to increase to 23 million tonnes by 2035 [41]. Moreover, ongoing efforts to enhance the process and reduce energy requirements highlight the potential of thermal plasma-assisted pyrolysis as an intriguing option for low-carbon hydrogen production.

In the subsequent chapter, a process simulation based on the fundamental principles of this technology will be developed, followed by an extensive economic evaluation and environmental impact assessment. These assessments will provide a comprehensive understanding of the overall performance of the plasma-assisted natural gas pyrolysis process in comparison to other existing hydrogen production technologies.

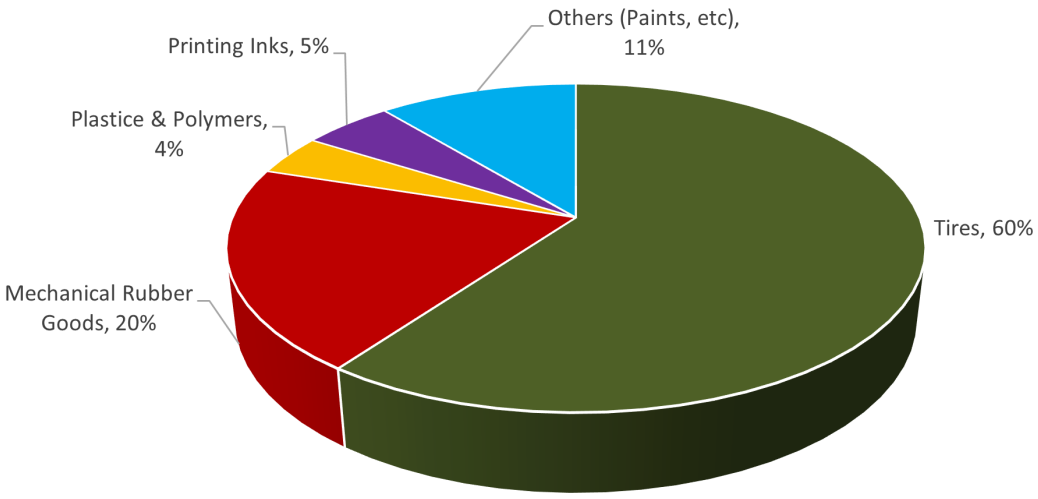


Figure 2.4: Carbon black market share by end user by volume (2021)[41]

# Chapter 3

# Process Simulation, Economics, and Environmental Impact Assessment

This chapter focuses on the process simulation of plasma-assisted natural gas pyrolysis (PNGP), along with an assessment of its economic viability and environmental impact. The chapter begins by presenting the methodology used to develop the process simulation, including the assumptions made regarding feed composition, operating conditions, and reaction kinetics. The simulation results provide valuable insights into the material and energy flows within the process, as well as the specific energy requirement and overall process efficiency for hydrogen production. Following the simulation, the chapter delves into the economic evaluation of the process, analyzing factors such as capital investment, operating costs, and potential revenue streams. Additionally, a comprehensive environmental impact assessment is conducted to evaluate the environmental footprint of the process, considering factors such as greenhouse gas emissions, resource consumption, and waste generation. Through these analyses, the chapter aims to provide a holistic understanding of the feasibility and sustainability of plasma-assisted natural gas pyrolysis as a promising technology for hydrogen production.

## 3.1 Process Simulation

### 3.1.1 Principles and Assumptions

The current section presents a methodology for developing a process simulation of plasma-assisted natural gas pyrolysis (PNGP) and conducting mass and energy balance calculations using Aspen Plus® software. The simulation results will be utilized to assess the environmental impact and economic aspects of the process.

Peng-Robinson is used as the primary thermodynamic property method in the simulation while Solids is used for solid handling equipment. The PNGP process simulation involves the utilization of a natural gas feedstock, with the composition outlined in Table 3.1. The feed is assumed to be at 30 bar and ambient temperature as the battery limit conditions of natural gas from transmission pipelines. The primary product of interest is gaseous hydrogen, expected to be generated at 20 bar and ambient temperature. Additionally, pelletized carbon black is considered the process's by-product. the process is also expected to produce undesirable products mainly in the form of off-quality carbon black and Coke [42].

Table 3.1: Natural gas composition used in the process simulation

| **Component** | **Mole Fraction** | **Component** | **Mole Fraction** |
|---|---|---|---|
| Methane | 0.95 | i-Pentane | 0.0001 |
| Ethane | 0.032 | n-Pentane | 0.0001 |
| Propane | 0.002 | Carbon Dioxide | 0.005 |
| i-Butane | 0.0003 | Nitrogen | 0.01 |
| n-Butane | 0.0003 | Oxygen | 0.0002 |

An attempt has been made to develop a comprehensive process simulation based on available data for the technology under investigation. The process simulation encompasses the following key sections.

**Natural Gas Pyrolysis -** This section includes the plasma reactor, heat integration equipment, gas/solid filters, and hydrogen product purification. The reactor is set to operate near-ambient pressure, as elevated pressures are unnecessary for plasma-assisted pyrolysis to occur [43]. The reaction temperature is set to 1800°C [43], which falls within the range of 1000 to 2500°C reported by

Fincke et al. as the temperature range where hydrogen and solid carbon are the predominant equilibrium products [34]. The reaction temperature is achieved by utilizing hot plasma gas, which is taken from the hydrogen-rich gas stream exiting the gas/solid filters. Aspen Plus® does not include any arrangement for a plasma reactor nor for plasma generating equipment. Thus, to simulate the plasma reactor the plasma gas is heated using a heater to heat up the gas to the desired plasma gas temperature (i.e., 3200°C) before sending it to the reactor to mix with the feed gas. The heater duty is used to estimate the power requirement of the plasma torch using the efficiency values presented in Table 3.2. To enhance the accuracy of the chemical mechanism within the reactor, a methane decomposition reaction mechanism proposed by Kozlov and Knorre [44] is employed. This mechanism comprises a set of reactions involving $CH_4$, $C_2H_6$, $C_2H_4$, $C_2H_2$, $H_2$, and $C$. The specific reactions are as follows:

$$CH_4(g) \xrightarrow{k_1} \frac{1}{2}C_2H_6(g) + \frac{1}{2}H_2(g) \tag{4}$$

$$C_2H_6(g) \xrightarrow{k_2} C_2H_4(g) + H_2(g) \tag{5}$$

$$C_2H_4(g) \xrightarrow{k_3} C_2H_2(g) + H_2(g) \tag{6}$$

$$C_2H_2(g) \xrightarrow{k_4} 2C(s) + H_2(g) \tag{7}$$

$k_1$, $k_2$, $k_3$, and $k_4$ are rate constants and given by the following equations:

$$k_1 = 4.5 \times 10^{13} \exp\left(\frac{-91000}{RT}\right) \tag{8}$$

$$k_2 = 9.1 \times 10^{13} \exp\left(\frac{-69000}{RT}\right) \tag{9}$$

$$k_3 = 2.57 \times 10^{8} \exp\left(\frac{-40000}{RT}\right) \tag{10}$$

$$k_4 = 1.7 \times 10^{6} \exp\left(\frac{-30000}{RT}\right) \tag{11}$$

where $R$ is the universal gas constant and $T$ is the temperature in Kelvin. For components other than methane in the feed, the calculation of phase and chemical equilibrium is performed using Gibbs free energy minimization as these components are also expected to decompose to hydrogen

and carbon under the above-mentioned reactor operating conditions. This is due to the lower energy required for the decomposition of these components compared to methane, which can be attributed to methane's stronger carbon-hydrogen bonds. Based on what has been discussed so far on the reactor, the reactor is chosen to be a hybrid of a plug flow and a Gibbs reactor where the plug flow reactor is used for methane employing the above-mentioned reaction mechanism while the Gibbs reactor is utilized for other hydrocarbons.

In terms of heat integration equipment, block heat exchangers are employed to facilitate the cooling of the reactor effluent and heating of the feed and recycled hydrogen gas used as plasma gas [45]. These heat exchangers are constructed using materials such as graphite, silicon carbide, or high-temperature ceramics, which can withstand temperatures exceeding 1000°C [45]. This design choice aims to decrease the electrical demand per kilogram of the product by sending hotter plasma gas to the plasma torch, thereby reducing the amount of electricity required for heating it to its final temperature [45]. To effectively separate carbon particles from hydrogen gas, high-efficiency baghouse filters are utilized. Meanwhile, the purification of hydrogen is accomplished through pressure swing adsorption beds.

**Carbon black processing -** The section dedicated to carbon black processing encompasses the processes of carbon black degassing, pelletizing, and drying. During this stage, hydrogen and other combustible gases trapped within the pores of the produced carbon black are removed by flowing the carbon black in a counter-current flow of an inert gas, such as nitrogen, which facilitates the extraction of the trapped gases [46]. Carbon black pelletizing is achieved using a water-based mixture containing a binder to agglomerate the carbon black particles into pellets [36]. For the drying process, an indirect fired rotary dryer is employed. This dryer operates by using an external source of heat to raise the temperature within the dryer. The carbon black is dried to a temperature of approximately 250°C within the dryer [36].

**Electricity generation through waste heat recovery -** To maximize energy recovery, the effluent from the reactor is subjected to additional cooling in a waste heat boiler, resulting in the production of steam. This steam is subsequently utilized in a Rankine cycle to generate electricity. Additionally, before entering the reactor, the natural gas feedstock undergoes depressurization to near ambient pressure using a turboexpander, which serves as an additional means of electricity

generation.

Table 3.2 summarizes key parameters utilized and the main assumptions made in the process simulation.

Table 3.2: Key parameters and main assumptions of the process simulation

| | | |
|---|---|---|
| **Plasma torch characteristics** | | |
| | Torch Efficiency | 0.90 [47] |
| | Thermal Efficiency | 0.95 [31] |
| **Compressors/Turbines** | | |
| | Isentropic Efficiency | 0.80 |
| | Mechanical Efficiency | 0.90 |
| **Pumps** | | |
| | Efficiency | 0.75 |
| **Gas/Solid Filters** | | |
| | Gas Separation Efficiency | 0.97 |
| | Solid Separation Efficiency | 1.00 |
| **Hydrogen PSA** | | |
| | Hydrogen recovery | 0.86 [48] |

### 3.1.2 Process Description

A schematic diagram outlining the process is presented in Figure 3.1. The initial step involves depressurizing the natural gas feedstock to 2 bar using a turboexpander where the released energy is used to generate electricity. Subsequently, the feed is combined with a hydrocarbon recycle stream rejected from the hydrogen purification section (PSA beds). The resulting mixture is then heated to 700°C, cooling the reactor effluent prior to entering the plasma reactor.

The reactor, operating at 1.7 bar, consists of two distinct regions: the plasma and the reaction zones, interconnected by a narrower section known as the throat. Within the plasma zone, plasma torches utilize a portion of the recycled hydrogen-rich gas from the downstream gas/solid filters to generate hot plasma gas at a temperature of 3200°C. The feed is introduced into the reactor through the throat, where it is mixed with plasma gas. Subsequently, the feed/plasma gas mixture enters the reaction zone at approximately 1800°C where the feed undergoes decomposition, primarily producing hydrogen and carbon nanoparticles.

The effluent stream from the reactor undergoes cooling, reaching temperatures around 670°C, by passing through the plasma gas preheater and the feed preheater, respectively. It is then directed

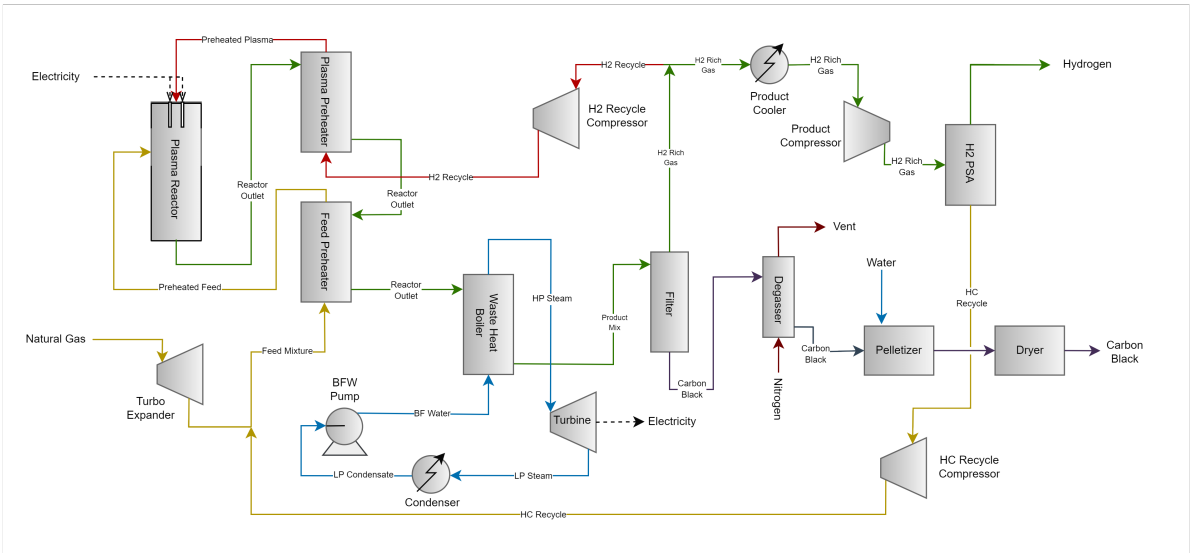


Figure 3.1: Plasma-assised natural gas pyrolysis flow diagram

to the waste heat boiler, where additional cooling takes place, reducing the temperature to approximately 180°C and generating steam. This steam is employed in electricity generation through a Rankine cycle.

The reactor effluent subsequently proceeds to the filtration section, where carbon particles are separated from the hydrogen-rich gaseous product. The separated carbon particles then undergo degassing in the downstream unit to eliminate the combustible gases trapped within their pores, utilizing a counter-current nitrogen stream. Following this, the carbon particles undergo pelletization and drying processes to produce carbon black.

A fraction of the hydrogen-rich gas derived from the filters is recycled and utilized as plasma gas. This gas is preheated to approximately 1150°C in the plasma preheater before being directed to the plasma torches to generate hot plasma gas.

The remaining portion of the hydrogen-rich gas is compressed and sent to the hydrogen purification section. In this section, hydrogen is separated from the unreacted gases utilizing a pressure swing adsorption (PSA) system equipped with appropriate molecular sieve beds. The rejected stream from the PSA system, containing unreacted hydrocarbons and hydrogen, is compressed and recycled, thereby mixed with the inlet feedstock stream. A flow diagram of the process in more detail has been provided in Appendix A.

### 3.1.3 Simulation Results

Table 3.3 provides an overview of the material and energy flows within the process. It indicates that the production of one kilogram of hydrogen necessitates 231.2 $MJ, LHV$ of natural gas as the primary feedstock, while concurrently yielding approximately 3 $kg$ of carbon black as a byproduct.

Based on the simulation results, the electricity generation in the system is calculated to be 1.4 $kWh/kgH_2$, while the process itself is estimated to consume 17.6 $kWh/kgH_2$. The main consumer of electricity is plasma generation equipment, accounting for approximately 83% of the total consumption (Figure 3.2). Additionally, other utility consumptions include 4.6 $m^3$ of nitrogen for carbon black degassing, 3.5 $kg$ of process water for carbon black pelletizing, and 0.4 $kg$ of deionized water as makeup water for the Rankine cycle.

Table 3.3: Material and energy flows of PNGP process

| | | | |
|---|---|---|---|
| **Input** | | | |
| | Natural Gas | $MJ, LHV/kgH_2$ | 231.2 |
| | | $kg/kgH_2$ | 4.78 |
| | Process Water | $kg/kgH_2$ | 3.5 |
| | Deionized Water | $kg/kgH_2$ | 0.4 |
| | Nitrogen | $m^3/kgH_2$ | 4.6 |
| | Electricity | $kWh/kgH_2$ | 17.6 |
| **Output** | | | |
| | Hydrogen | $kg$ | 1.0 |
| | Carbon Black | $kg/kgH_2$ | 3.0 |
| | Carbon, Other | $kg/kgH_2$ | 0.5 |
| | Electricity | $kWh/kgH_2$ | 1.4 |

The natural gas (methane) conversion per pass of the reactor is estimated to be approximately 95%. By recycling the rejected stream from hydrogen PSA back to the reactor inlet, the overall conversion of the process reaches around 99.5%.

With the findings mentioned above, the specific energy requirement for the process is determined to be 16.2 $kWh/kgH_2$, while the overall process efficiency in terms of hydrogen production is calculated using equation 12 to be 41.4%.

$$eff(\%) = \frac{m_{H2} \times LHV_{H2}}{E_T + m_{NG} \times LHV_{NG}} \times 100 \tag{12}$$

where $m$ is the mass flow rate, $LHV$ is the lower heating value, and $E_T$ is the total energy demand

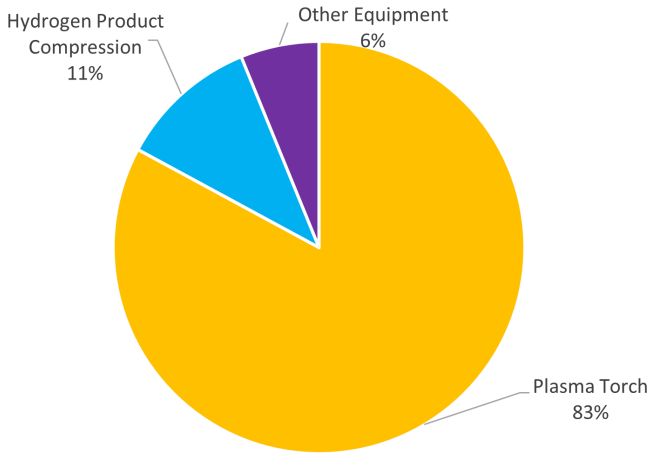


Figure 3.2: Electricity consumption breakdown of PNGP process

of the process.

## 3.2 Process Economics

This section focuses on assessing the financial viability and competitiveness of the plasma-assisted natural gas pyrolysis process. In this section, key assumptions and the methodology employed for cost estimation are presented. Capital costs, including equipment procurement, installation, and infrastructure development, are estimated based on industry benchmarks. Operating costs, encompassing raw material expenses, utilities, maintenance, and labor, are evaluated to provide a comprehensive understanding of the ongoing expenses associated with the process. Eventually, the minimum selling price of hydrogen is estimated by considering various factors, including capital and operating costs, production capacity, and projected market demand. By examining these economic aspects, this section aims to provide valuable insights into the financial feasibility and potential profitability of the proposed hydrogen production process.

### 3.2.1 Assumptions

Table 3.4 presents the fundamental assumptions and parameters employed in the economic evaluation of the hydrogen production process. The operating time factor is assumed to be 90%. Considering the total annual hours of 8760, the plant's annual operation hours will be 7884 hours. The economic analysis is conducted for a plant with a production capacity of 100 tonnes per day of hydrogen which is considered a midsize plant needed to provide the hydrogen requirement of a petroleum refinery with a capacity of around 100,000 barrels of crude per day. The evaluation is conducted for the year 2021, with all monetary values expressed in US Dollars. To determine the feasibility and profitability of the process, key factors such as feedstock and utility prices are taken into account and presented in Table 3.5. Notably, the process generates carbon black as a byproduct, and its potential revenue is considered in the calculations, assuming a market price of 0.4 USD per kilogram.

Table 3.4: Economic evaluation assumptions

| **Parameter** | **Value** |
|---|---|
| Plant Lifetime (yr) | 30 |
| Capacity Factor (%) | 90 |
| Operating Factor (%) | 90 |
| Annual Operation Time (hr) | 8760 |
| Currency | USD |
| Estimation Year | 2021 |
| CEPCI | 708.8 [49] |
| Construction Period (yr) | 3 |
| Loan Lifetime (yr) | 15 |
| Loan Interest Rate (%) | 5 |
| Federal & Provincial Tax Rate (%) | 26 |
| Debt Ratio (%) | 40 |
| IRR (%) | 10 |
| Inflation Rate (%) | 3 |
| Depreciation | 7-year |
| Number of Operating Shifts | 5 |
| Labour Wage (USD/person-hr) | 25 [50] |

Table 3.5: Feedstock and utility prices

| **Item** | **Price** |
|---|---|
| Natural Gas ($USD/GJ$) | 6 |
| Electricity ($USD/kWh$) | 0.06 |
| Nitrogen ($USD/m^3$) | 0.03 |
| Deionized Water ($USD/tonne$) | 1.36 |
| Process Water ($USD/tonne$) | 0.66 |

### 3.2.2 Capital Investment Costs

The majority of the equipment costs used as reference costs have been estimated using Aspen Process Economic Analyzer (APEA) software, while costs of certain equipment such as the plasma reactor and hydrogen purification PSA beds have been obtained from the relevant literature. To account for variations in equipment size and the estimation year, Equation 13 is employed to update the costs,

$$Cost = Cost_{Ref} \times (\frac{Capacity}{Capacity_{Ref}})^n \times (\frac{CEPCI}{CEPCI_{Ref}}) \tag{13}$$

where it incorporates a scaling factor denoted by $n$ and the chemical engineering plant cost index ($CEPCI$). For the present analysis, the cost estimation year is designated as 2021, with a corresponding $CEPCI$ value of 708.8. The scaling factor ranges between 0.6 and 1, depending on the specific equipment being considered.

Once the purchased equipment costs have been established, the total capital investment cost (CAPEX) can be determined using the factors outlined in Table 3.6. Furthermore, the annualized CAPEX is calculated by multiplying the CAPEX value by an annualization factor, denoted by $AF$. The calculation of $AF$ is accomplished using Equation 14,

$$AF = \frac{i(1+i)^N}{(1+i)^N - 1} \tag{14}$$

wherein $i$ represents the interest rate, and $N$ signifies the number of years.

Table 3.6: Capital investment cost factors used for CAPEX estimation [51, 52]

| **Cost Parameter** | **Value** | |
|---|---|---|
| Delivery Cost | 8% | of purchased equipment cost |
| **Direct Costs (% of Equipment Delivered Costs)** | | |
| Installation Costs | | |
| Equipment Erection | 40% | |
| Piping | 70% | |
| Instrumentation | 20% | |
| Electrical | 10% | |
| Utility Cost | 10% | |
| Off-sites | 20% | |
| Buildings | 20% | |
| Site Preparation | 10% | |
| Land | 6% | |
| **Indirect Costs (% of Equipment Delivered Costs)** | | |
| Engineering and Supervision | 22% | |
| Construction Overhead | 18% | |
| Project Contingency | 10% | of Fixed Capital Investment |
| **Fixed Capital Investment (FCI) = Direct Costs + Indirect Costs** | | |
| Startup Costs | 9% | of Fixed Capital Investment |
| Working Capital | 15% | of Total Capital Investment |
| **Total Capital Investment (TCI) = Fixed Capital Investment + Startup Costs + Working Capital** | | |

### 3.2.3 Operating Costs

The operating costs associated with the process encompass several components, including the expenditure on raw materials and utilities necessary for the operation. Additionally, fixed operating costs such as labor, maintenance, overhead costs, property insurance, taxes, and general expenses are taken into account. The estimation of raw material and utility costs is based on the results obtained from the process simulation. Labor wages are determined by considering factors such as plant size and type, labor wage rate, number of shifts, and the total number of operators per shift. The equation provided in Perry's Chemical Engineers Handbook [53] is employed for this purpose. Other operating costs can be estimated using the factors outlined in Table 3.7. The total operating cost is then calculated by summing up all the aforementioned costs, providing a comprehensive assessment of the ongoing expenses incurred during the process.

Table 3.7: Operating costs factors used for OPEX estimation [54, 53]

| **OPEX Parameter** | **Value** | |
|---|---|---|
| Operating Labor Costs | | |
| Labor Wages | Calculated from [53] | |
| Supervision & Engineering | 22% | of Labor Wages |
| Operating Supplies & Services | 6% | of Labor Wages |
| Laboratory Expenses | 15% | of Labor Wages |
| Payroll Charges | 35% | of Labor Wages + Supervision & Engineering |
| Maintenance Costs | | |
| Maintenance Wages | 3.5% | of FCI (Excluding Land) |
| Maintenance Supervision & Engineering | 25% | of Maintenance Wages |
| Material Supplies | 100% | of Maintenance Wages |
| Maintenance Overhead | 5% | of Maintenance Wages |
| Overhead Costs | | |
| Plant Overhead | 7.1% | of TWSE* |
| Mechanical Department Services | 2.4% | of TWSE* |
| Employee Relations Department | 5.9% | of TWSE* |
| Business Services | 7.4% | of TWSE* |
| Property Insurance & Taxes | 2% | of FCI |
| General Expenses | | |
| Sale Expenses | 3% | of Sales |
| Research & Development | 5% | of Sales |
| Administrative Expenses | 3% | of Sales |

*TWSE is the total of labor and maintenance wages and supervision & engineering costs

### 3.2.4 Economic Evaluation

Figure 3.3 provides the breakdown of the purchased equipment costs associated with a plasma-assisted natural gas pyrolysis plant of $100 tonnes/day$ hydrogen production capacity. A detailed cost breakdown has been presented in Appendix A. The analysis reveals that the plasma reactor cost constitutes approximately 65% of the total equipment cost, primarily attributed to the expenses related to plasma torches. It is noteworthy that despite advancements in the manufacturing of plasma torches, this aspect remains a significant area for potential improvement in terms of process capital investments. In contrast, the carbon black processing section exhibits the lowest proportion of equipment cost, suggesting that the development of the byproduct production section has a relatively minor influence on the overall capital investments of the plant.

Table 3.8 provides a comprehensive overview of the economic performance of a natural gas

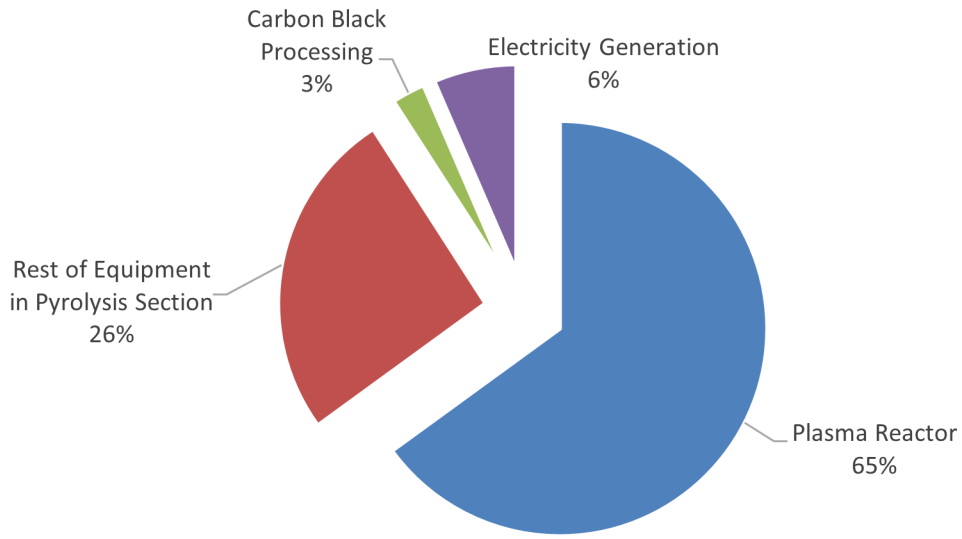


Figure 3.3: Equipment cost breakdown of the plasma-assisted natural gas pyrolysis (PNGP)

pyrolysis plant with a hydrogen production capacity of 100 tonnes per day. The evaluation encompasses two distinct scenarios, one including the capital and operating costs as well as revenues associated with carbon black production (i.e., Scenario 1), and the other excluding them from the overall economic analysis (i.e., Scenario 2). The estimated minimum selling price of hydrogen is calculated to be 3.5 USD/kg for Scenario 1 and 4.5 USD/kg for Scenario 2. It is noteworthy that although both investment and operating costs are lower for Scenario 2, the minimum selling price of hydrogen derived for this Scenario is higher. This observation suggests that carbon black revenues have a substantial impact on the process, outweighing its production costs, as the production of one kilogram of hydrogen results in approximately three kilograms of carbon black generation. Moreover, the analysis reveals that over 60% of the total operating costs of the process are attributed to the expenses incurred for raw materials and utilities, particularly natural gas and electricity. This finding underscores the significance of these two input costs in determining the final price of the hydrogen product.

The economic evaluation of the natural gas pyrolysis process revealed key insights into the production costs and pricing of hydrogen. The breakdown of purchased equipment costs demonstrated

Table 3.8: Economic performance of plasma-assisted natural gas pyrolysis

| **Parameter** | **Unit** | **Scenario 1**[a] | **Scenario 2**[b] |
|---|---|---|---|
| Hydrogen Production | tonne/day | 100 | |
| Carbon Black Byproduct | tonne/day | 295 | 0 |
| **Purchased Equipment Cost** | **MMUSD** | **55.3** | **53.7** |
| Total Direct Costs | MMUSD | 182.9 | 177.5 |
| Total Indirect Costs | MMUSD | 46.9 | 45.5 |
| Fixed Capital Investment | MMUSD | 229.8 | 223.0 |
| **Total Capital Investment** | **MMUSD** | **294.7** | **286.0** |
| **Annualized CAPEX** | **MMUSD/yr** | **26.2** | **25.4** |
| **Operating Costs** | **MMUSD/yr** | **113.7** | **108.6** |
| Raw Materials & Utility | MMUSD/yr | 72.2 | 68.6 |
| Other Operating Costs | MMUSD/yr | 41.5 | 40 |
| **Hydrogen Minimum Selling Price** | **USD/kg** | **3.5**[c] | **4.5** |

[a]Scenario 1: Economic evaluation including carbon black-related costs and revenues
[b]Scenario 2: Economic evaluation excluding carbon black-related costs and revenues
[c]Calculated assuming carbon black market price of 0.4 USD/kg

that the plasma reactor, primarily comprising plasma torches, accounts for a significant portion of the total equipment cost, indicating potential room for improvement in capital investments. Conversely, the carbon black processing section had a relatively small share of the equipment cost, suggesting that the development of the byproduct production section does not heavily impact capital investments. The economic performance analysis for two scenarios, with and without considering carbon black production costs and revenues, highlighted the influence of carbon black revenues on the process. Despite lower investment and operating costs in Scenario 2, the minimum selling price of hydrogen was lower in Scenario 1, indicating the significant impact of carbon black revenues. Additionally, raw materials and utility costs, mainly natural gas and electricity prices, constituted a considerable portion of the total operating costs, emphasizing their importance in determining the final price of the hydrogen product. A comprehensive analysis of the economic outcomes will be presented in Chapter 4, where a comparative assessment of prices will be conducted, taking into account alternative methods of hydrogen production. Additionally, sensitivity analyses will be performed to examine the key factors influencing the economic aspects of the process. This detailed investigation aims to provide a deeper understanding of the economic viability of plasma-assisted natural gas pyrolysis and identify the primary contributors to its economic performance.

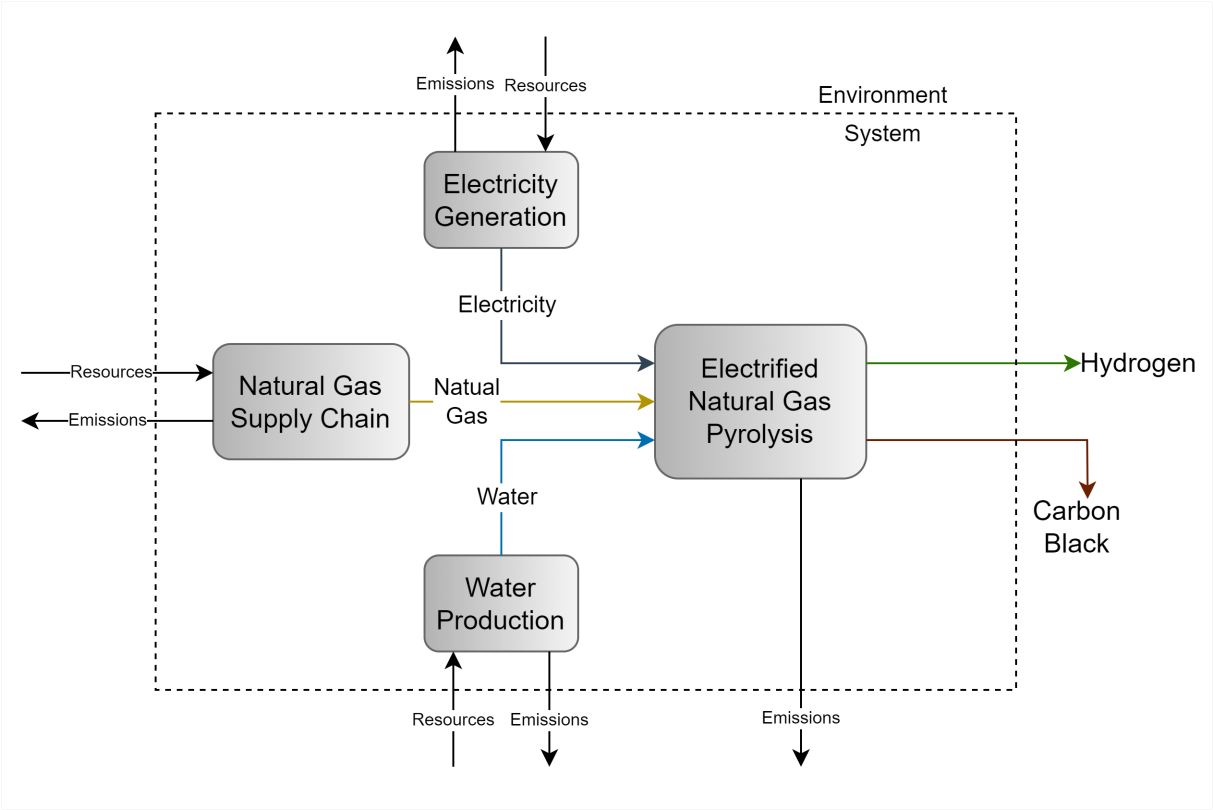


Figure 3.4: Plasma-assisted natural gas pyrolysis system boundary

## 3.3 Environmental Impact Assessment of the Process

The environmental impact assessment section of this study aims to evaluate the environmental performance of the plasma-assisted natural gas pyrolysis (PNGP) process throughout its entire life cycle. By assessing key environmental indicators such as greenhouse gas emissions, energy consumption, and resource utilization, this section provides valuable insights into the environmental sustainability of PNGP as a hydrogen production method.

Figure 3.4 illustrates the cradle-to-gate boundary for hydrogen production through plasma-assisted natural gas pyrolysis. The functional unit adopted for the calculations is one kilogram of hydrogen product. The study focuses on a plant located in Canada, with British Columbia as the primary case, while Alberta, Ontario, and Quebec are also analyzed for comparative purposes. Additionally, the evaluation encompasses the influence of various electricity generation sources on the system, considering six different resources: coal, hydro, natural gas, nuclear, solar, and wind.

Table 3.9: Plasma-assisted natural gas pyrolysis process inputs/outputs

| | | |
|---|---|---|
| **Inputs** | | |
| | Natural Gas $(Nm^3)$ | 6.83 |
| | Electricity $(kWh)$ | 16.20 |
| | Water $(kg)$ | 3.84 |
| **Outputs** | | |
| | Products | |
| | Hydrogen $(kg)$ | 1.00 |
| | Carbon Black $(kg)$ | 2.95 |
| | Emissions | |
| | Carbon Dioxide $(g)$ | 35.12 |
| | Carbon Monoxide $(g)$ | 5.94 |
| | Methane $(g)$ | 7.54 |
| | Other Hydrocarbons $(g)$ | 0.38 |
| | Nitric Oxide $(g)$ | 11.22 |
| | Dinitrogen Monoxide $(g)$ | $7.6 \times 10^{-4}$ |
| | Nitrogen Dioxide $(g)$ | $4.0 \times 10^{-3}$ |

Furthermore, incorporating carbon black production credits as a byproduct of plasma-assisted natural gas pyrolysis involves recognizing carbon black as an avoided product produced through the conventional method of Furnace Black as the most common method of carbon black production. This consideration leads to two scenarios: one including carbon black production credits in the estimations and another excluding such credits. The Furnace Black data are extracted from the ecoinvent database and include all upstream facilities' impacts.

The potential direct emissions and resource requirements of the natural gas pyrolysis process, as obtained from the process simulation results, are presented in Table 3.9. Environmental impact assessment results are estimated using the ReCiPe 2016 method in the OpenLCA software. The method provides characterization factors that are representative of the global scale and can perform the impact assessment at both midpoint and endpoint levels with eighteen midpoint and three endpoint indicators. Using the same method at both levels enhances the consistency in the development of midpoint and endpoint levels. Version 3.8 of the ecoinvent database is utilized to source the necessary data on the natural gas supply chain including natural gas production and its transportation via pipeline, electricity generation, and water production. System characteristics and assumptions for different defined scenarios are outlined in Table 3.10. The reference processes from the ecoinvent database used in the environmental impact assessment of the system under different scenarios

are listed in Table 3.11.

## 3.4 Summary

Chapter 3 of this thesis focused on the comprehensive analysis of plasma-assisted natural gas pyrolysis (PNGP) as a hydrogen production method. The chapter began by describing the process simulation of PNGP, detailing the main assumptions and principles, operating conditions, and material and energy flows. The subsequent sections delved into the economic evaluation and environmental impact assessment of the PNGP process. The economic evaluation involved estimating capital and operating costs, as well as determining the minimum selling price of hydrogen. The impact assessment examined the environmental performance of PNGP, considering indicators such as greenhouse gas emissions, energy consumption, and resource usage. The results of these analyses will be presented in chapter 4, where they will be compared against other hydrogen production methods, and sensitivity analyses will be conducted to identify the main contributors to the process economics and environmental impacts.

Table 3.10: System characteristics and assumptions for different scenarios

| **Scenarios Based on Geographical Location** | |
|---|---|
| **Scenario** | **Characteristics** |
| Alberta | - Natural gas production in Alberta<br>- Electricity provided from Alberta grid |
| British Columbia | - Natural gas production in BC<br>- Electricity provided from BC grid |
| Ontario | - Natural gas production in Alberta<br>- Natural gas pipeline transport of 3000 km from Alberta to Ontario<br>- Electricity provided from Ontario grid |
| Quebec | - Natural gas production in Alberta<br>- Natural gas pipeline transport of 4000 km from Alberta to Quebec<br>- Electricity provided from Quebec grid |
| **Scenarios Based on Electricity Source** | |
| **Scenario** | **Characteristics** |
| Coal Electricity | High voltage electricity production in a hard coal power plant |
| Hydro Electricity | Equal shares of high voltage electricity production in a reservoir and a run-of-river power plant |
| NG Electricity | High voltage electricity production in a combined cycle natural gas power plant |
| Nuclear Electricity | High voltage electricity production in a pressurized heavy water reactor nuclear plant |
| Solar Electricity | High voltage electricity production in a central tower solar power plant |
| Wind Electricity | High voltage electricity production in an onshore wind power plant |

Table 3.11: List of reference processes from ecoinvent database version 3.8

| **Product Name** | **Reference Process** | **Location** | **Process UUID** |
|---|---|---|---|
| electricity, high voltage | electricity, high voltage, production mix \| electricity, high voltage \| APOS, S | Canada, Alberta | 9a6c39c5-fd90-3551-b5b3-52714844ae30 |
| | electricity, high voltage, production mix \| electricity, high voltage \| APOS, S | Canada, British Columbia | 808d59d3-18c5-3974-bc9a-151f3ee67cb2 |
| | electricity, high voltage, production mix \| electricity, high voltage \| APOS, S | Canada, Ontario | caa52796-faf9-397b-b7c1-fa1fa91e7918 |
| | electricity, high voltage, production mix \| electricity, high voltage \| APOS, S | Canada, Quebec | b0f863e6-5542-3b70-a932-cf18903aa825 |
| natural gas | natural gas production \| natural gas, high pressure \| APOS, S | Canada, Alberta | bf716741-b66c-39ae-b123-d5411e1f7b10 |
| | transport, pipeline, long distance, natural gas \| transport, pipeline, long distance, natural gas \| APOS, S | Rest-of-World | bfda758c-7467-3a21-9493-6a16a534757c |
| carbon black | carbon black production \| carbon black \| APOS, S | Global | b214357f-ed6b-3f3d-aced-06f6a361aa01 |
| water, deionised | water production, deionised \| water, deionised \| APOS, S | Rest-of-World | 23f6767c-24d3-4c1a-8831-0f023f1e2333 |

# Chapter 4

# Results and Evaluation

## 4.1 Introduction

Chapter 4 of this thesis presents the results and evaluation of plasma-assisted natural gas pyrolysis (PNGP) in comparison to other prevalent methods of hydrogen production, namely steam methane reforming (SMR) and water electrolysis. This chapter critically examines and compares these different methods' efficiency, economics, and environmental performance. The evaluation encompasses a comprehensive analysis of critical parameters, including hydrogen production efficiency, capital and operating costs, and environmental impact indicators such as greenhouse gas emissions and resource consumption. The chapter builds upon the process simulation, economic evaluation, and environmental impact assessment conducted in Chapter 3, where the PNGP process was studied in detail. The results obtained from Chapter 3 will be presented and thoroughly analyzed in this chapter, providing valuable insights into the performance of PNGP compared to SMR and water electrolysis. Furthermore, sensitivity analyses will be conducted to investigate the main contributors to process economics, enhancing our understanding of the economic viability of PNGP. The results will also be compared to existing methods and technologies in order to assess the potential of PNGP as a sustainable and efficient hydrogen production method.

## 4.2 Results Evaluation

### 4.2.1 Process Efficiency

Figure 4.1 provides a comparative analysis of the energy efficiency results for plasma-assisted natural gas pyrolysis (PNGP) in comparison to steam methane reforming (SMR), SMR coupled with carbon capture and storage (CCS), and proton exchange membrane (PEM) electrolysis. The efficiencies are determined using Equation 12, considering the lower heating values of the natural gas feed and hydrogen product. The process data for calculating the efficiencies of SMR, SMR+CCS, and PEM electrolysis are obtained from the H2A: Hydrogen Analysis Production Models developed by the National Renewable Energy Laboratory (NREL) [55]. As observed from the figure, SMR exhibits the highest efficiency at 71.7%. However, incorporating a carbon capture and storage section in the SMR process leads to a reduction in efficiency of over 6%. The efficiency of PEM electrolysis is estimated at 60% for an electrolyzer with a power consumption of 55 $kWh/kgH_2$. In comparison, PNGP demonstrates the lowest efficiency among the evaluated methods. When compared to SMR, PNGP consumes more natural gas and electricity per kilogram of hydrogen produced, with a portion of the energy originally contained in the natural gas being stored as carbon. Moreover, Although PNGP exhibits lower electricity consumption than electrolysis, its utilization of natural gas as a feedstock, coupled with its electricity requirements, results in lower energy efficiency compared to the electrolysis process.

### 4.2.2 Economics

Figure 4.2 illustrates the variation in the minimum selling price of hydrogen with respect to plant capacity, ranging from 20 $tonnes/day$ to 500 $tonnes/day$ of hydrogen production. Notably, the price reduction is more significant for smaller plant sizes, with about a 20% decrease observed from a capacity of 20 $tonnes/day$ to 100 tonnes/day. However, the price reduction becomes less pronounced as plant capacity increases, with only an 8% reduction from a 100 $tonnes/day$ plant to a $500 tonnes/day$ plant. This trend can be attributed to the impact of reactor cost, which serves as the primary contributor to capital expenditure (CAPEX) and it is assumed to increase with a scaling factor of one.

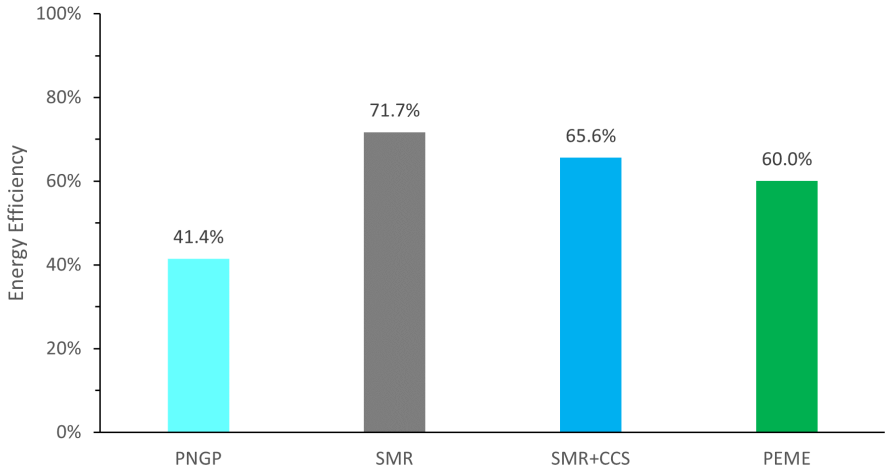


Figure 4.1: Energy efficiency in terms of hydrogen production. SMR, SMR+CCS, and PEME results extracted from [55]

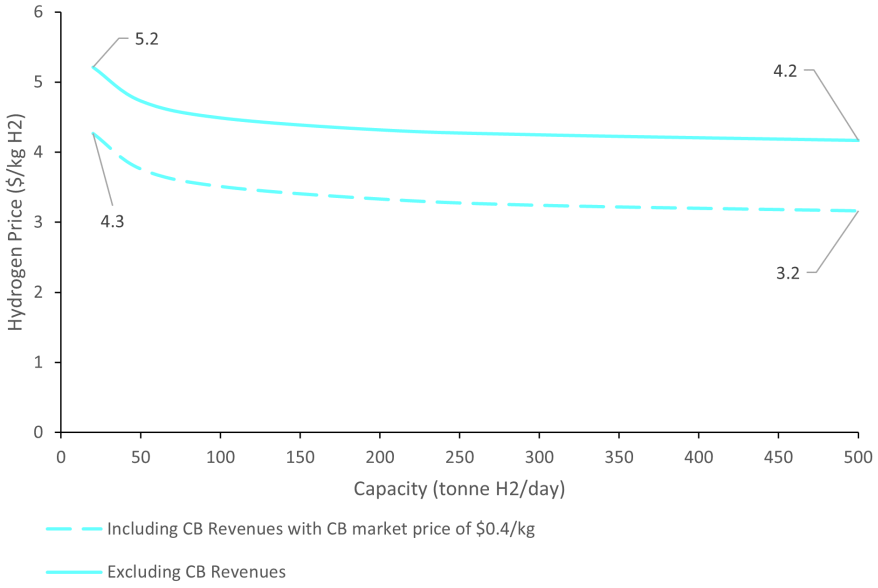


Figure 4.2: Hydrogen minimum selling price sensitivity to the plant capacity (natural gas price: $\$6/GJ$; electricity price: $\$0.06/kWh$)

To assess the economic viability of plasma-assisted natural gas pyrolysis (PNGP), the minimum selling price of hydrogen produced by the process is compared to prices obtained from steam methane reforming (SMR), SMR coupled with carbon capture and storage (CCS), and proton exchange membrane (PEM) electrolysis. To ensure a consistent comparison, the cost estimation calculations for SMR, SMR with CCS, and PEM electrolysis follow the same assumptions and methodology described in Section 3.2, with equipment costs obtained from NREL's H2A: Hydrogen Analysis Production Models [55]. The production capacity is set at 300 $tonnes/day$ to align with the scaling limits specified in the NREL models. Table 4.1 summarizes the characteristics of these technologies.

Table 4.1: SMR, SMR with CCS, and water electrolysis system characteristics [55]

| **Hydrogen Production Technology** | **Main Characteristics** |
|---|---|
| Steam Methane Reforming (SMR) | Natural gas requirement: 166 $MJ_{LHV}/kgH_2$<br>Electricity requirement: 0.13 $kWh/kgH_2$ |
| Steam Methane Reforming with Carbon Capture and Storage (SMR+CCS) | Natural gas requirement: 177 $MJ_{LHV}/kgH_2$<br>Electricity requirement: 1.5 $kWh/kgH_2$<br>Carbon capture efficiency: 96%<br>$CO_2$ pipeline length: 160 $km$ |
| Water Electrolysis | Technology: PEM<br>Electricity requirement: 55.5 $kWh/kgH_2$ |

Figure 4.3 presents the hydrogen minimum selling prices for PNGP, SMR, SMR+CCS, and PEM electrolysis for a plant with a hydrogen capacity of 300 tonnes per day. PNGP demonstrates a selling price of $4.25 per kilogram of hydrogen, while SMR, SMR+CCS, and PEM electrolysis show prices of $1.87, $3.26, and $6.52, respectively. However, considering the inclusion of carbon black revenues based on a market price of $0.4/kg, the hydrogen price for PNGP reduces to $3.24, nearly matching the price of SMR+CCS. Although this price is half that of PEM electrolysis, PNGP still falls short when compared to SMR in terms of cost competitiveness.

Based on what has been discussed so far, one potential way for achieving economic competitiveness between plasma-assisted natural gas pyrolysis (PNGP) and steam methane reforming (SMR) is through the market price of carbon black. Figure 4.4 illustrates the variations in hydrogen selling price as a function of the carbon black market price. The figure reveals that PNGP's hydrogen price can rival that of SMR only if the carbon black market price reaches approximately $0.9/kg or higher. Additionally, the figure includes the average carbon black price in North America over the past three

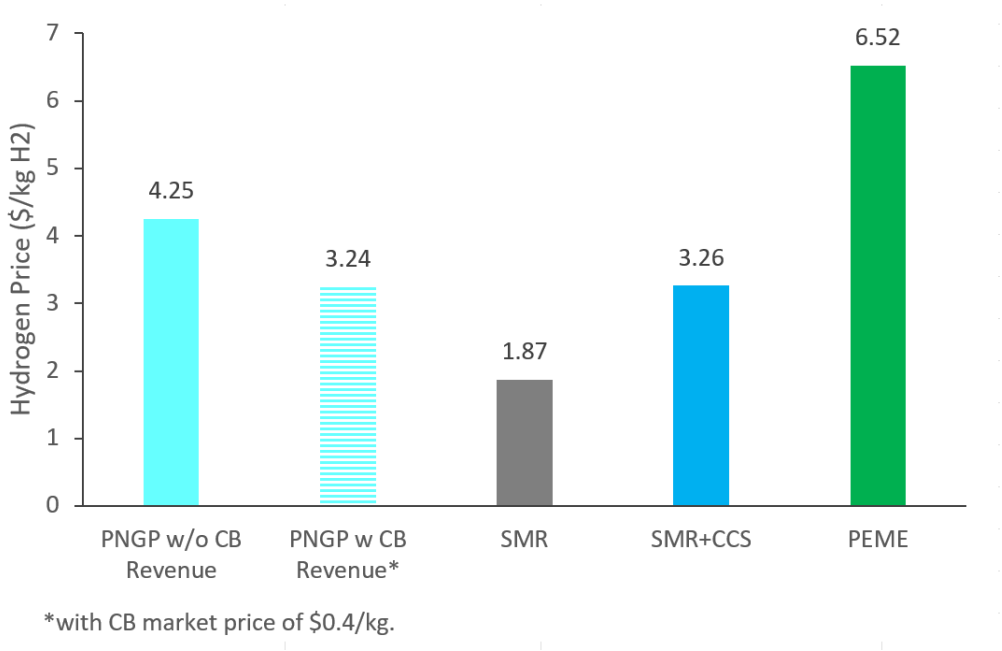


Figure 4.3: Hydrogen minimum selling price of PNGP compared to SMR and water electrolysis (capacity: 300 $tonnes H_2/day$; natural gas price: $\$6/GJ$; electricity price: $\$0.06/kWh$)

years [56], indicating an upward trend during this period, with the price peaking at $0.63/kg in the previous year.

Based on the simulation results discussed in Section 3.1.3, the net electricity requirement of plasma-assisted natural gas pyrolysis (PNGP) is estimated to be 16.2 $kWh/kgH_2$, which is significantly higher than the electricity requirement of steam methane reforming (SMR) plant. According to NREL's H2A: Hydrogen Analysis Production Models [55], the net electricity consumption of an SMR plant is reported to be approximately 0.13 $kWh/kgH_2$, and this value increases to around 1.5 $kWh/kgH_2$ when a $CO_2$ capture and storage section is added. The higher electricity demand of PNGP is a crucial factor impacting its economic performance. Figure 4.5 examines this influence by illustrating the variations in hydrogen prices produced from PNGP compared to other technologies (SMR, SMR+CCS, and PEME) as a function of electricity prices.

As observed in the figure, PEM electrolysis is the most sensitive to electricity prices, as it requires the highest amount of electricity. It is worth noting that PEME cannot compete with SMR at any electricity price, while it only matches the SMR+CCS hydrogen price for electricity prices

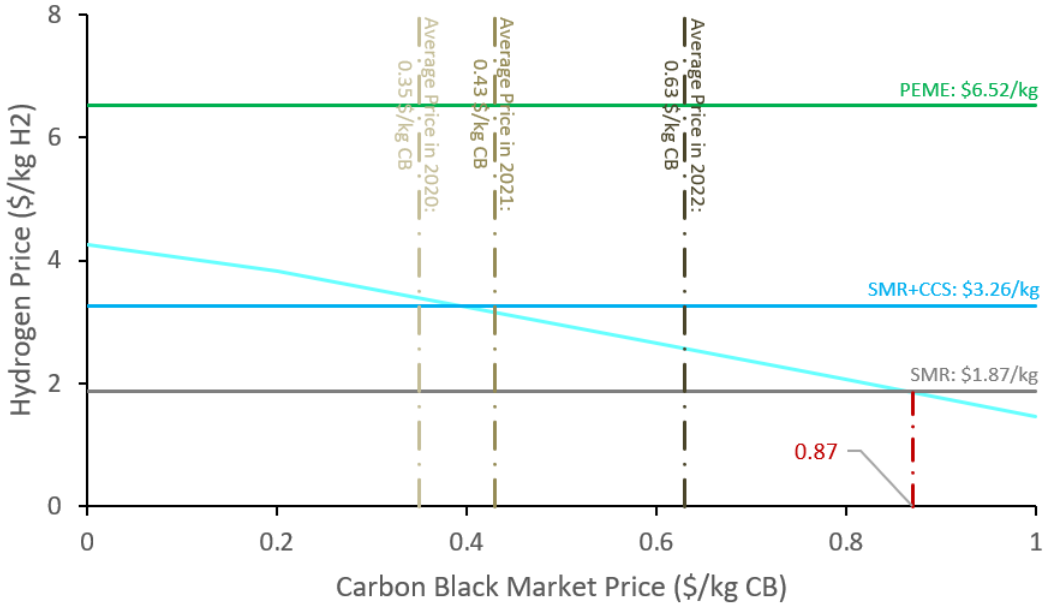


Figure 4.4: Effect of carbon black market price on hydrogen selling price (capacity: 300 $tonnes H_2/day$; natural gas price: $\$6/GJ$; electricity price: $\$0.06/kWh$)

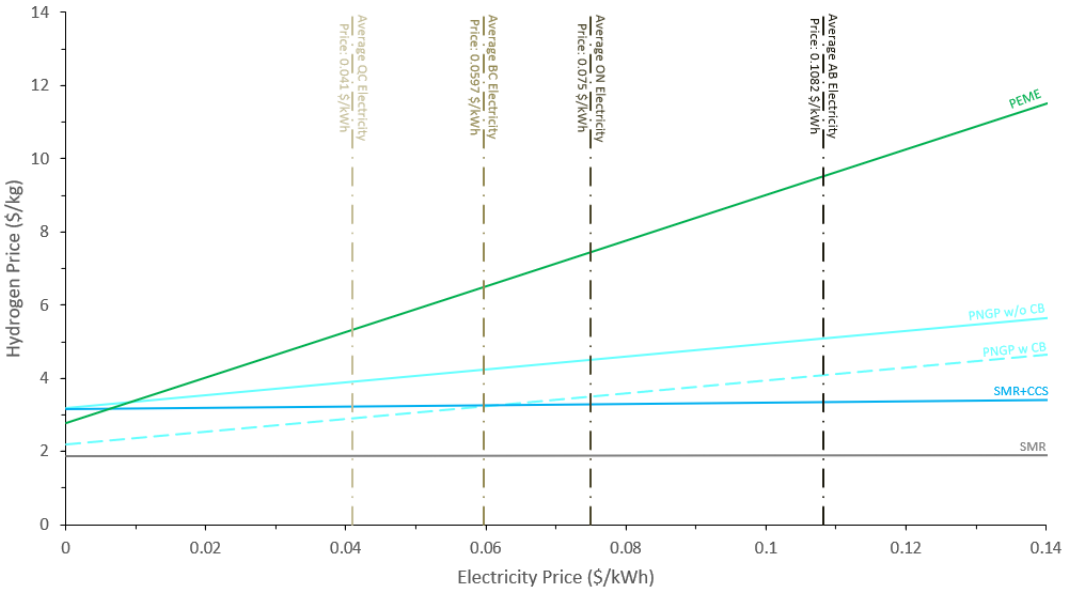


Figure 4.5: Hydrogen selling price as a function of electricity price (capacity: 300 $tonnes H_2/day$; natural gas price: $\$6/GJ$; carbon black market price: $\$0.4/kg$)

below $\$0.01/kWh$. Conversely, both SMR and SMR+CCS show minimal sensitivity to electricity prices, as hydrogen prices remain relatively stable across a wide range of electricity prices. PNGP falls between these two extremes, unable to surpass SMR at any electricity price even when considering carbon black revenues of $\$0.4/kg$ in the calculations. Nevertheless, PNGP outperforms SMR+CCS for electricity prices below $\$0.06/kWh$. Additionally, the figure displays the average industrial electricity prices of four Canadian provinces (Alberta, British Columbia, Ontario, and Quebec), with Quebec having the lowest price at $\$0.041/kWh$ and Alberta having the highest at approximately $\$0.11/kWh$ [57]. This suggests that the financial competitiveness of the PNGP process would be higher if located in British Columbia or Quebec, rather than Ontario or Alberta.

Natural gas is another significant factor influencing the economic performance of the PNGP process. PNGP consumes approximately 230 $MJ$ of natural gas per kilogram of hydrogen produced, whereas the natural gas consumption for SMR and SMR+CCS is around 166 $MJ/kgH_2$ and 177 $MJ/kgH_2$, respectively [55]. Figure 4.6 demonstrates the relationship between hydrogen price and natural gas price for the PNGP process compared to other hydrogen production technologies. Notably, PEM electrolysis is not sensitive to natural gas prices as it does not utilize natural gas as a feedstock. In the comparison between PNGP and SMR, the price of hydrogen produced by PNGP exhibits a steeper increase as natural gas prices rise due to its higher consumption rate. PNGP does not surpass the performance of SMR at any natural gas price, but it becomes competitive with SMR+CCS when natural gas prices fall below $\$6/GJ$. This falls within North America's average natural gas price range reported for 2022 [58]. Additionally, it is worth mentioning that the PEME hydrogen price falls short of surpassing SMR in the natural gas price range of \$0 to $\$25/GJ$. Still, it can compete with SMR+CCS and PNGP at natural gas prices exceeding $\$20/GJ$ and $\$15/GJ$, respectively.

### 4.2.3 Environmental Impact Assessment

The environmental impacts of plasma-assisted natural gas pyrolysis (PNGP) are assessed using the ReCiPe 2016 method for both midpoint and endpoint analyses. These results are compared to the impacts of steam methane reforming (SMR), SMR with carbon capture and storage (CCS), and PEM electrolysis. NREL's H2A: Hydrogen Analysis Production Models [55] and GREET® 2022

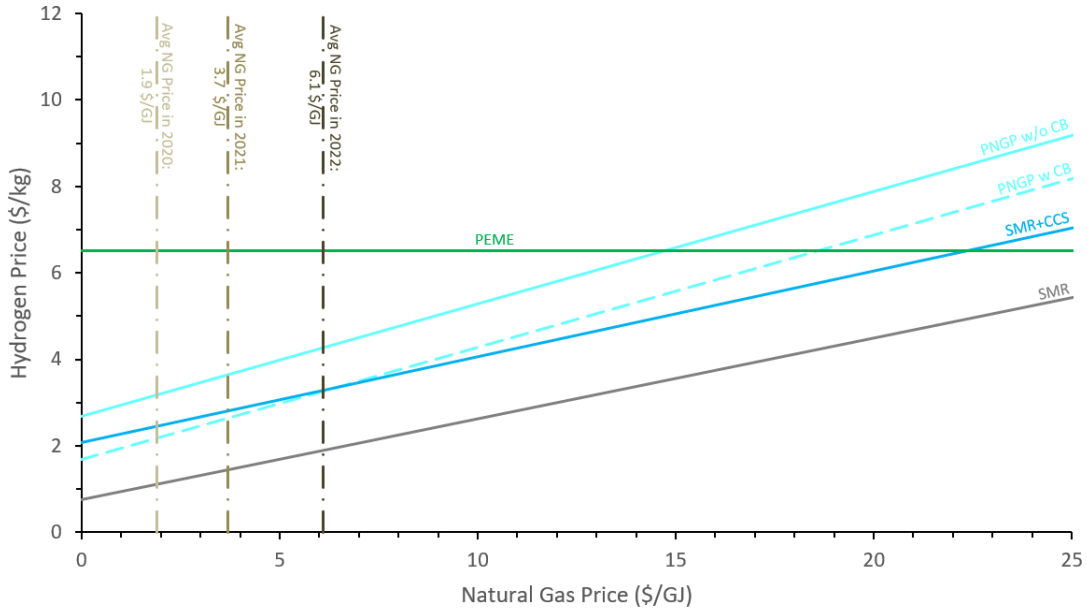


Figure 4.6: Hydrogen selling price as a function of natural gas price (capacity: 300 $tonnes H_2/day$; electricity price: $\$0.06/kWh$; carbon black market price: $\$0.4/kg$)

[59] were utilized to obtain these technologies' process and emission data, respectively. To ensure a consistent evaluation, the electricity generation and natural gas supply chain processes used in the PEM electrolysis, SMR, and SMR with CCS systems were matched with those employed in PNGP.

Given that the PNGP process consumes a significant amount of electricity compared to SMR, the source of electricity is expected to have a substantial influence on PNGP's environmental impacts. Figure 4.7 displays the contribution of each process to the total greenhouse gas (GHG) emissions of the PNGP system under six different scenarios of electricity generation. Additionally, the emissions from an SMR plant are included for comparison. The contributions of the pyrolysis process, natural gas supply chain, and carbon black production remain consistent across all six scenarios, with only electricity generation being variable. Notably, while the pyrolysis process itself is not a major contributor to total emissions, the choice of electricity source can significantly impact its emissions. Thus, it can be inferred that the PNGP process achieves acceptable emission levels only when coupled with renewable or nuclear electricity. Moreover, from the figure, it is observed that carbon black production yields negative emission values in the calculations. This is because carbon black is

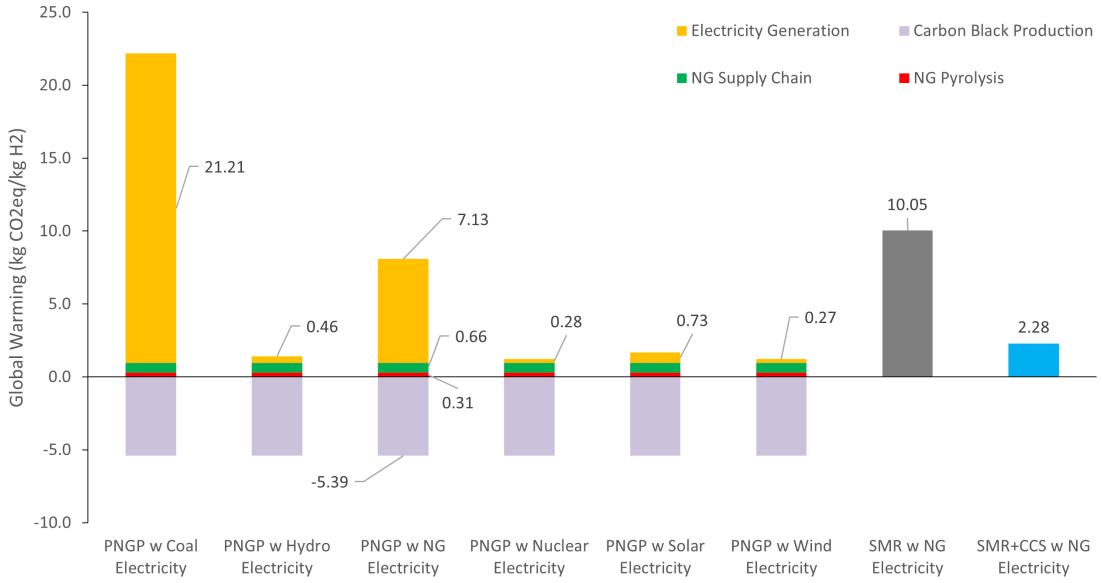


Figure 4.7: PNGP system's process impact contribution to system's total GHG emissions under different electricity generation scenarios

considered an avoided product in the system, indicating that its production as a byproduct of PNGP reduces the emissions associated with its production through other processes (i.e., the Furnace Black Process). The influence of carbon black production on the environmental impact of PNGP will be further examined by comparing the results when carbon black production is included versus when it is excluded from the system.

The midpoint impact results of PNGP, considering both the inclusion and exclusion of carbon black production credits (PNGP w CB and PNGP w/o CB, respectively), are compared to the results of SMR and SMR with CCS in Figures 4.8, 4.9, 4.10, and 4.11 across the six different electricity generation scenarios. While PNGP exhibits lower global warming impacts when coupled with renewable electricity, it tends to yield higher values in nearly all other impact categories compared to SMR and SMR with CCS. However, when the credits of carbon black production are included in the PNGP system, it achieves the most favorable results in the majority of categories. This clearly demonstrates the significant role of carbon black in enabling the system to attain environmentally acceptable impact levels compared to conventional hydrogen production technologies.

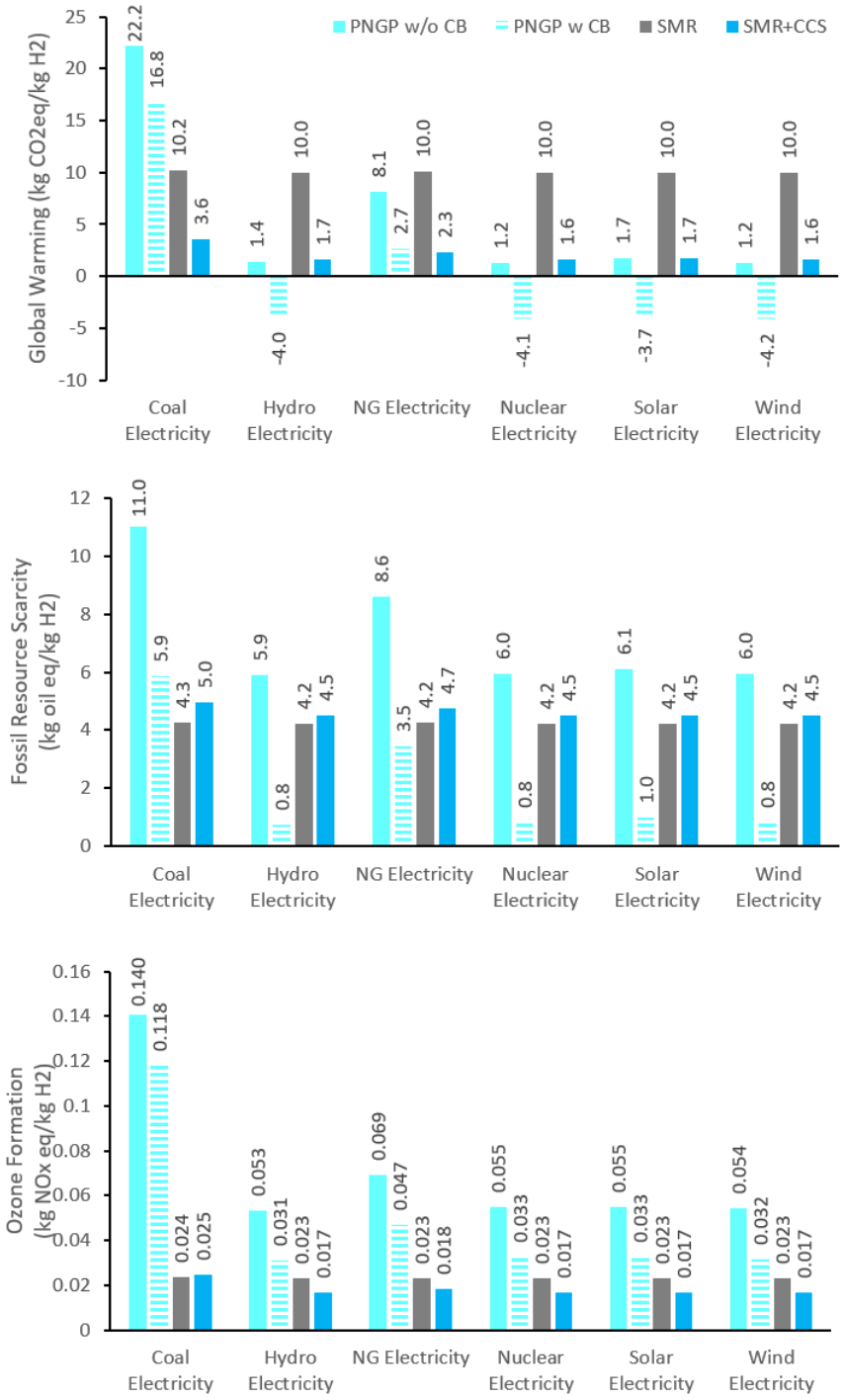


Figure 4.8: ReCiPe midpoint results under different electricity scenarios - part 1: global warming, fossil resource scarcity, and ozone formation; for ozone formation details see Appendix A

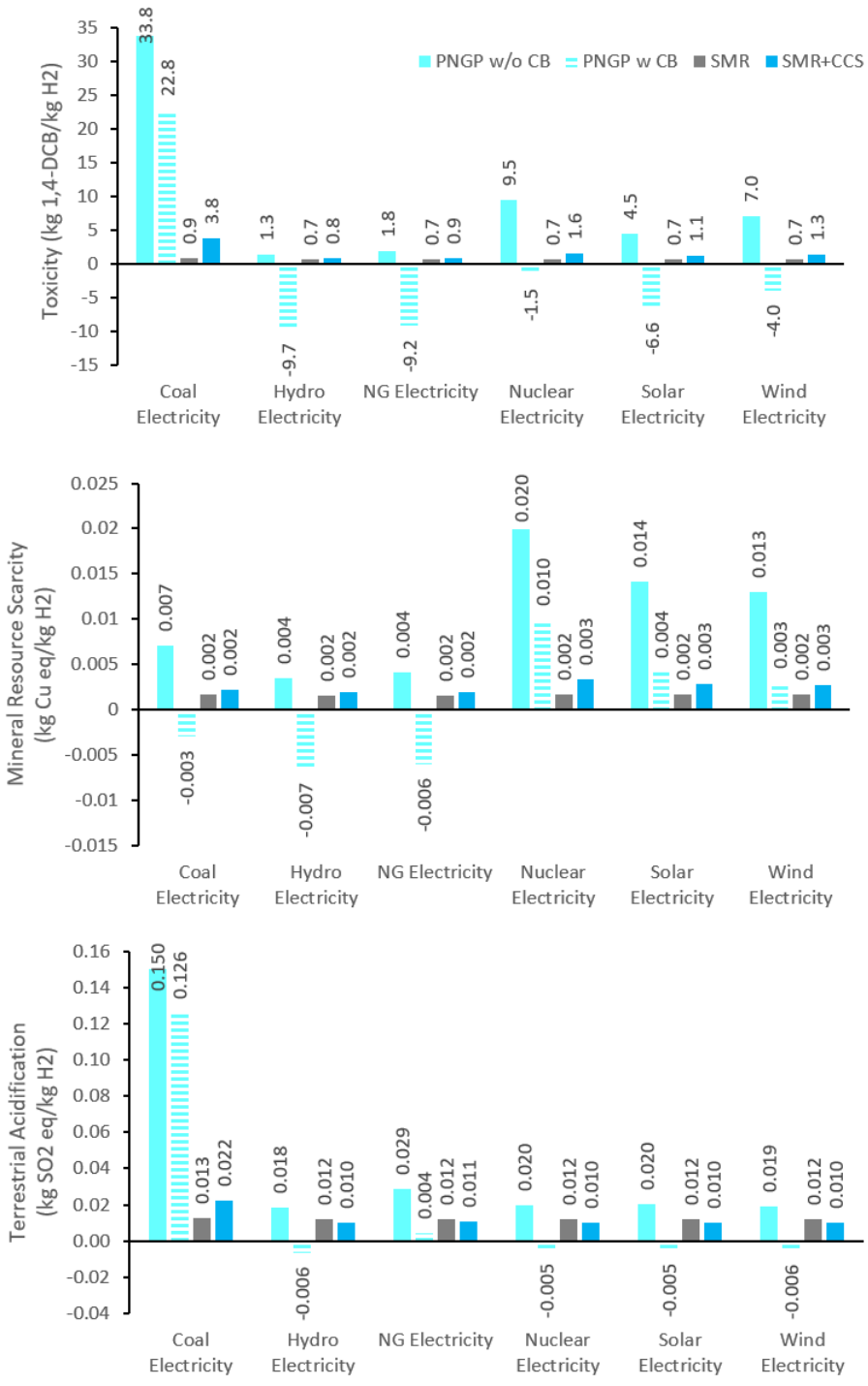


Figure 4.9: ReCiPe midpoint results under different electricity scenarios - part 2: toxicity, mineral resource scarcity, and terrestrial acidification; for toxicity details see Appendix A

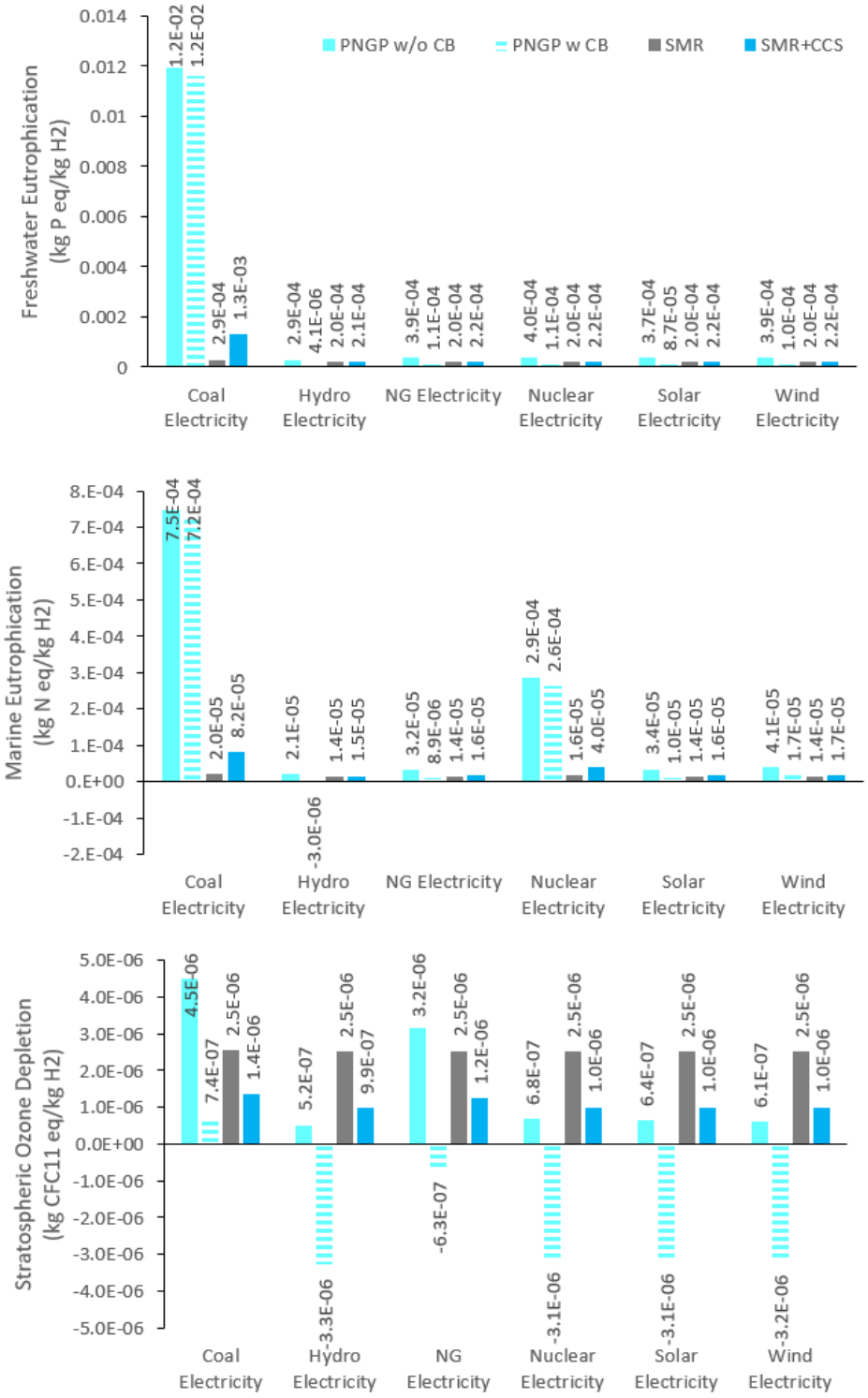


Figure 4.10: ReCiPe midpoint results under different electricity scenarios - part 3: freshwater eutrophication, marine eutrophication, and stratospheric ozone depletion

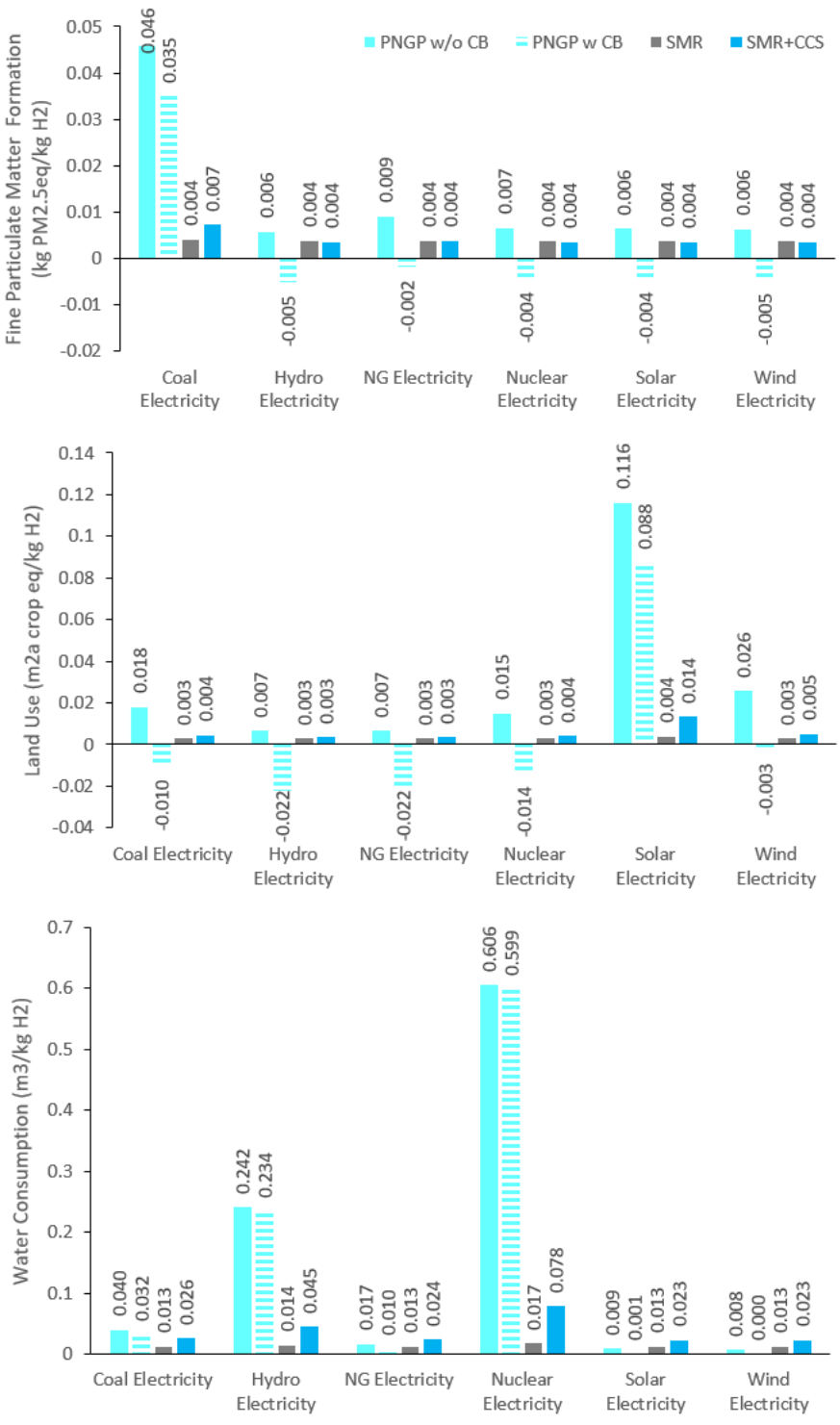


Figure 4.11: ReCiPe midpoint results under different electricity scenarios - part 4: fine particulate matter formation, land use, and water consumption

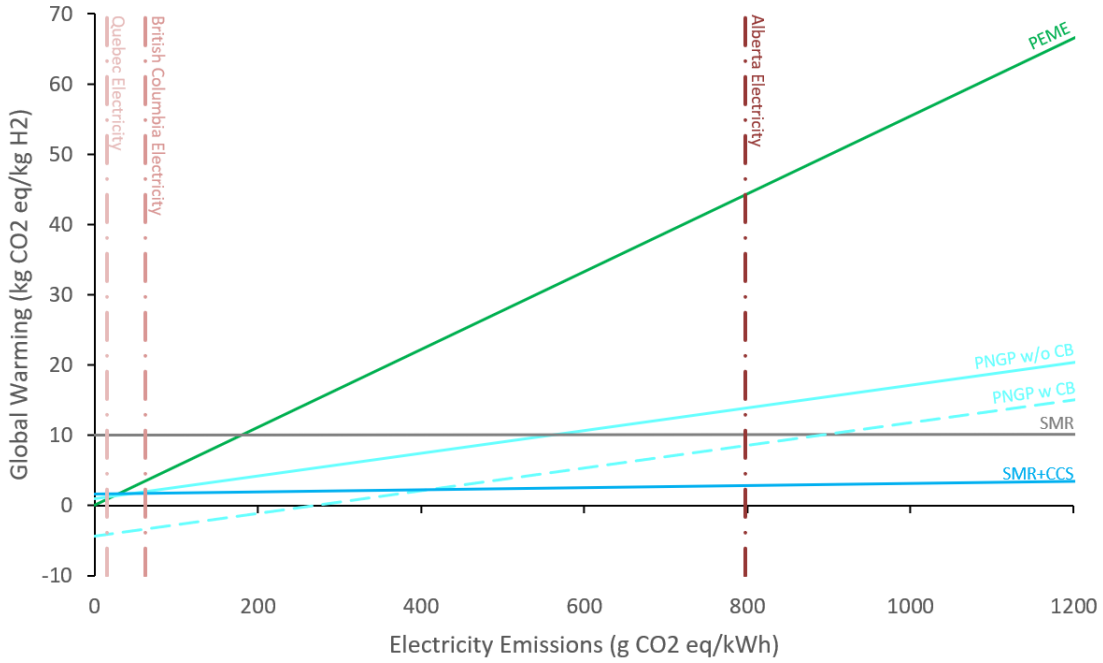


Figure 4.12: PNGP's GHG emissions as a function of electricity carbon footprints in comparison with other technologies

Figure 4.12 depicts the relationship between the global warming impact of PNGP, SMR, SMR with CCS, and PEM electrolysis, as influenced by electricity carbon footprints. SMR exhibits minimal sensitivity to electricity emissions, while SMR with CCS shows a slight increase in emissions. Conversely, both PNGP and PEM electrolysis experience substantial emissions growth, with PEM electrolysis exhibiting the steepest incline. From the figure, it can be inferred that SMR with CCS is the most favorable option for regions such as Alberta, where electricity emissions levels are high. Conversely, in provinces like Quebec and British Columbia, which predominantly generate renewable electricity, PNGP, with the inclusion of carbon black production credits, emerges as the most advantageous method. SMR with CCS, PEM electrolysis, and PNGP without carbon black credits display comparable performance in such regions.

So far, it has been demonstrated that the electricity source significantly influences the environmental impacts of PNGP, while carbon black production contributes to improved PNGP results compared to SMR and SMR+CCS. In order to gain a more comprehensive understanding of the system's environmental performance, an analysis is conducted considering geographical conditions.

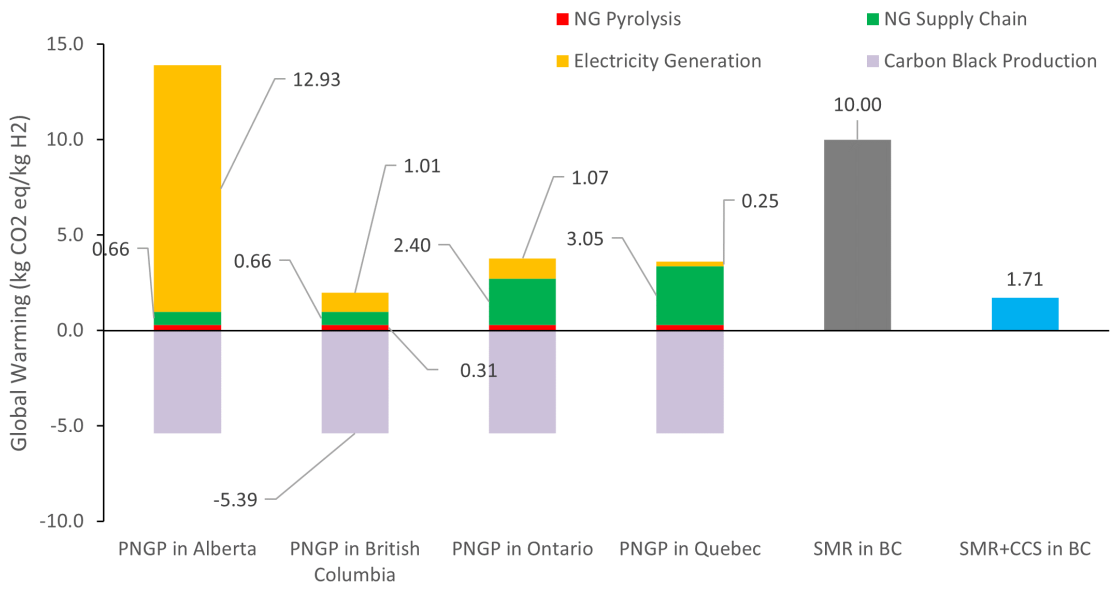


- Water production emissions are not presented as they are smaller than chart scale (≈0.001 kg $CO_2$ eq/kg $H_2$).

Figure 4.13: PNGP system's process impact contribution to system's total GHG emissions in four different privinces

Four scenarios are examined based on different provinces in Canada, as outlined in Table 3.10.

Figure 4.13 illustrates the contribution of the main processes to the global warming impact of the PNGP system in Alberta, British Columbia, Ontario, and Quebec, alongside the potential emissions level of an SMR process for comparison. Alberta is most affected by electricity emissions, while the impact is significantly lower in the other three provinces, with Quebec having the lowest electricity-related emissions. These findings align with the respective electricity source shares in each province, with approximately 89% of Alberta's electricity originating from fossil fuels in 2019, compared to less than 5% for British Columbia, around 7% for Ontario, and nearly zero for Quebec [60]. Conversely, the natural gas supply chain contributes most to the global warming impact in Ontario and Quebec, attributed to emissions associated with the pipeline transfer of natural gas due to the absence of domestic natural gas production in these provinces.

In summary, Figure 4.13 indicates that PNGP in Alberta exhibits emissions levels similar to the potential emissions of an SMR plant, while the other three locations result in significantly lower

emissions. Among these, British Columbia demonstrates the most favorable performance, benefiting from both low electricity emissions and reduced natural gas supply emissions. Therefore, a more detailed investigation of its environmental performance compared to other methods will be conducted hereinafter.

Figure 4.14 showcases the midpoint impact results of the PNGP system, considering both the inclusion and exclusion of carbon black production credits, in comparison with SMR with CCS technology. These results have been normalized using the midpoint impact results of SMR as a baseline. When the carbon black credit is not accounted for in the PNGP system, PNGP generally exhibits higher midpoint impact values compared to the SMR baseline process, with the exception of global warming and stratospheric ozone depletion impact categories. It is noteworthy to compare these findings with SMR with CCS technology, which generally yields lower impact values across all impact categories when compared to PNGP without carbon black production credits. SMR with CCS performs particularly well in particulate matter formation, global warming, ozone formation, stratospheric ozone depletion, and acidification categories where its impact results are lower compared to both SMR and PNGP. However, incorporating the carbon black production credits into the PNGP system significantly enhances its overall impact performance, where it scores negative values in several categories surpassing both SMR and SMR with CCS. Nevertheless, regardless of whether the carbon black production credits are included in the system or not, PNGP still demonstrates higher impact values in terms of water consumption, ozone formation, and land use when compared to the other technologies. The electricity generation process, which is a crucial component of the PNGP system, is the primary contributor to all those three categories.

Figure 4.15 displays the normalized endpoint impacts of PNGP, along with SMR with CCS using SMR impact values as a reference. Both cases of PNGP exhibit better results in terms of human health and ecosystem quality compared to SMR, with SMR with CCS falling between the two. However, the impacts of PNGP without carbon black credits and SMR with CCS are higher than those of the SMR baseline process in the resources category. This is attributed to the higher natural gas consumption per kilogram of hydrogen produced in both PNGP and SMR with CCS, as compared to SMR. On the other hand, incorporating carbon black credits into the PNGP system reduces resource consumption, as the same amount is now considered for both hydrogen and carbon

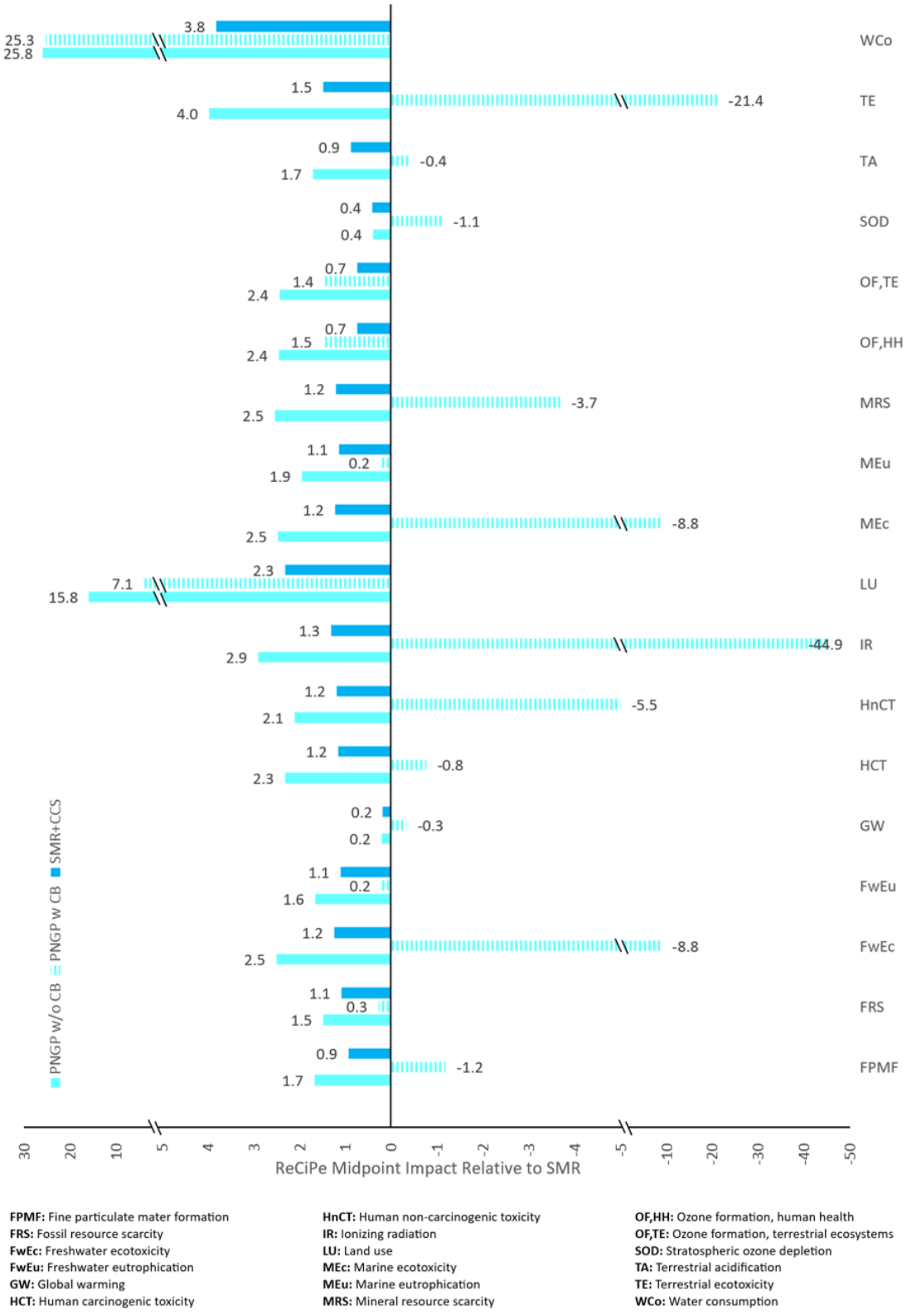


Figure 4.14: Normalized ReCiPe Midpoint Impacts of PNGP and SMR with CCS in BC, Canada; for detailed results see Appendix A

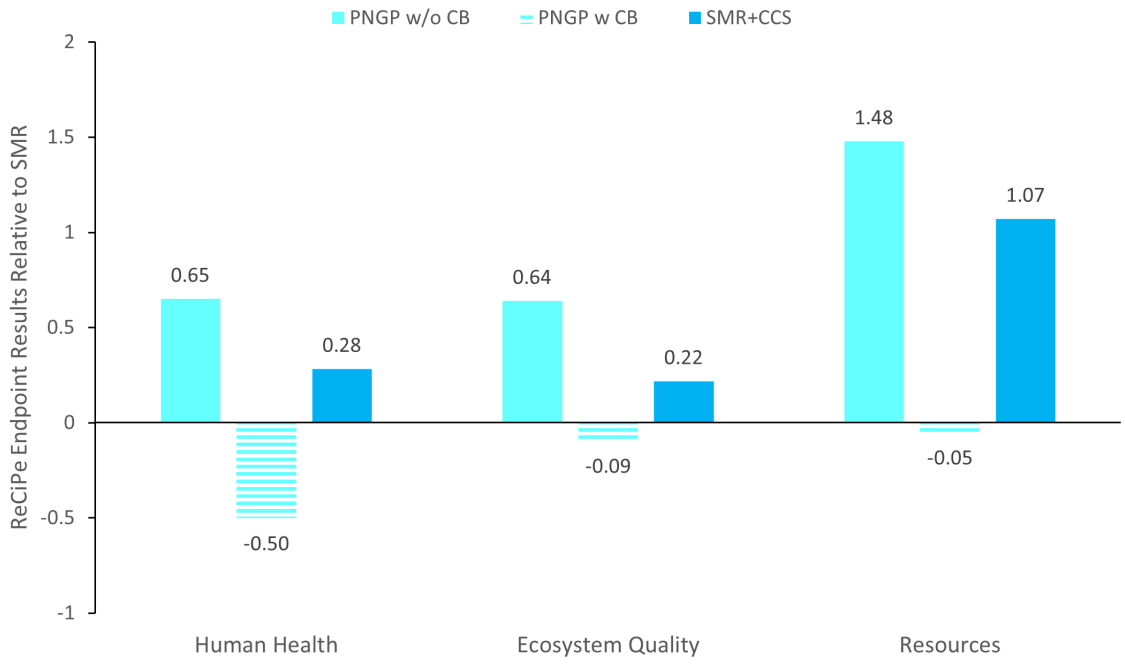


Figure 4.15: Normalized ReCiPe Endpoint Impacts of PNGP and SMR with CCS in BC, Canada

black production. In summary, the findings from the midpoint and endpoint impact assessments suggest that while electrified natural gas production must be coupled with renewable electricity to achieve acceptable environmental impacts compared to other hydrogen production technologies, it can outperform other low-carbon hydrogen production solutions like SMR with CCS when the credits for carbon black byproduct are considered in the system.

Based on the obtained results regarding the economic performance and environmental impacts of plasma-assisted natural gas pyrolysis in comparison to other hydrogen production methods, it is now possible to estimate and compare the cost of avoided greenhouse gas (GHG) emissions by the process with the cost of captured or avoided emissions from alternative technologies. Equation 15 is utilized for this estimation, as presented below:

$$C_{GHG} = \frac{MSP_T - MSP_{SMR}}{GHG_{SMR} - GHG_T} \tag{15}$$

where $C_{GHG}$ represents the cost of avoided or captured GHG emissions in US dollars per kilogram of $CO_2$ equivalent ($\$/kgCO_2eq$), $MSP_T$ and $MSP_{SMR}$ denote the hydrogen minimum selling prices in US dollars per kilogram of hydrogen ($\$/kgH_2$) for the target technology and SMR, respectively, and $GHG_T$ and $GHG_{SMR}$ indicate the GHG emissions in kilograms of $CO_2$ equivalent per kilogram of hydrogen ($kgCO_2eq/kgH_2$) for the target technology and SMR, respectively.

Figure 4.16 showcases the variations in the cost of avoided/captured emissions as a function of electricity price, while Figure 4.17 illustrates the changes in the cost of avoided/captured emissions as a function of natural gas price. Among the considered hydrogen production technologies, PEM electrolysis demonstrates the highest sensitivity to electricity prices, yielding competitive outcomes only when electricity prices fall below $\$0.01/kWh$. In comparison, SMR with CCS outperforms PNGP for all electricity price ranges when carbon black production credits are not included in the estimation. However, incorporating these credits leads to improved results for PNGP up to electricity prices of approximately $\$0.12/kWh$.

The impact of changes in natural gas prices on the cost of avoided or captured GHG emissions varies across different hydrogen production technologies. For PEM electrolysis, the cost is initially high at low natural gas prices but decreases as natural gas prices increase. However, PEM electrolysis can only compete with PNGP without carbon black credits when natural gas prices exceed $\$15/GJ$, and it requires further increases to approximately $\$25/GJ$ to outperform other technologies. Without considering carbon black production credits, PNGP cannot rival SMR with CCS at any natural gas prices. Nevertheless, incorporating these credits into the calculations allows PNGP to achieve the best results for natural gas prices up to around $\$23/GJ$.

To better understand the environmental impact of using natural gas pyrolysis for making hydrogen, we looked at a specific case where a petroleum refinery could switch from using steam methane reforming (SMR) to natural gas pyrolysis (PNGP) for producing hydrogen. Figure 4.18 presents the hydrogen requirement and total GHG emissions of a typical petroleum refinery. The data has been extracted from PRELIM [61], a petroleum refinery life cycle inventory model developed by the University of Calgary. The refinery processes about 100,000 barrels of crude oil per day and needs hydrogen for its operations. The data showed that the refinery requires around 128 tonnes of hydrogen daily, out of which SMR provides about 99 tonnes. The total greenhouse gas emissions from

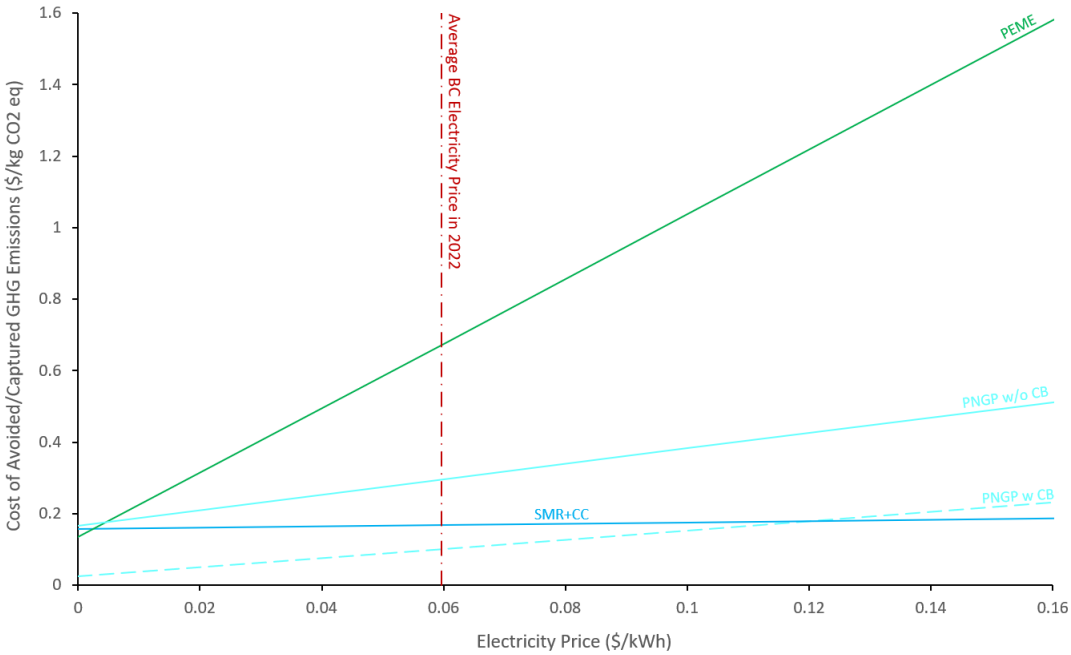


Figure 4.16: Cost of avoided/captured GHG emissions as a function of electricity price (capacity: 300 $tonnes H_2/day$; natural gas price: $\$6/GJ$; carbon black market price: $\$0.4/kg$)

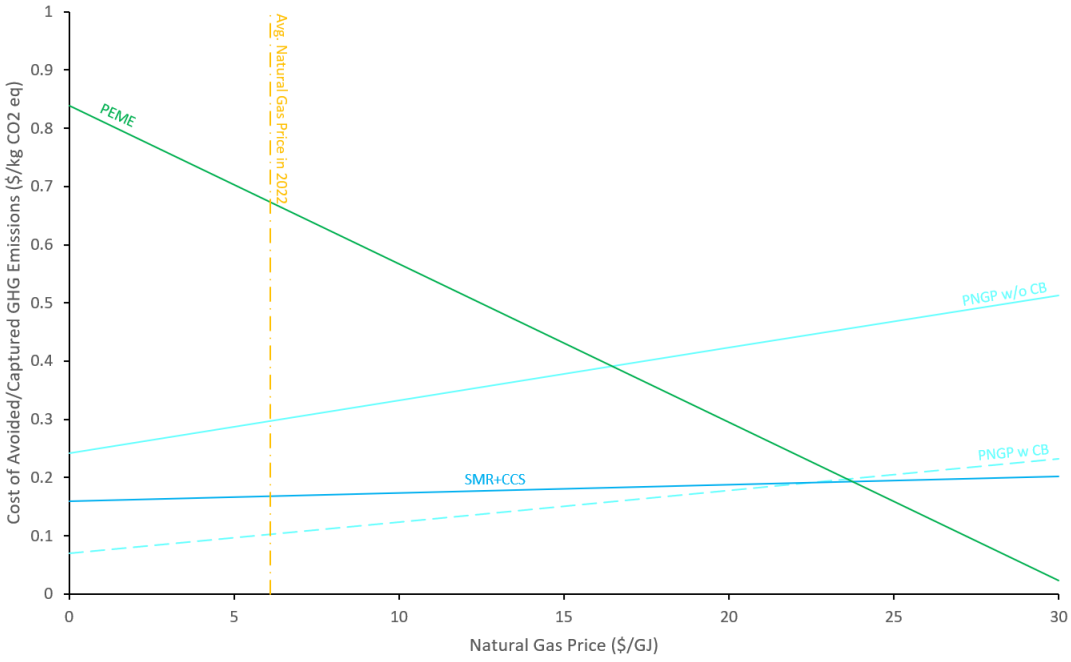


Figure 4.17: Cost of avoided/captured GHG emissions as a function of natural gas price (capacity: 300 $tonnes H_2/day$; electricity price: $\$0.06/kWh$; carbon black market price: $\$0.4/kg$)

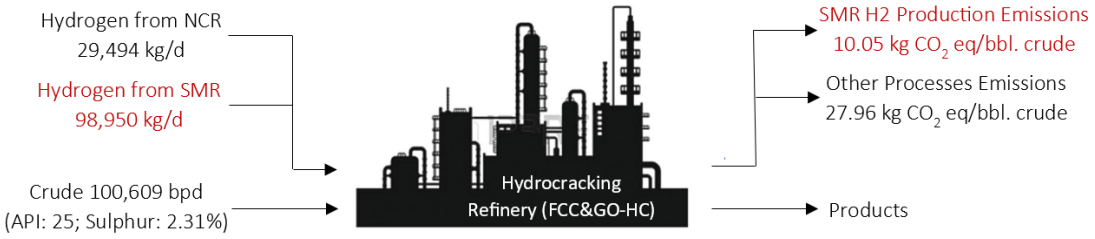


Figure 4.18: Hydrogen requirement and emissions of a typical hydrocracking refinery [61]

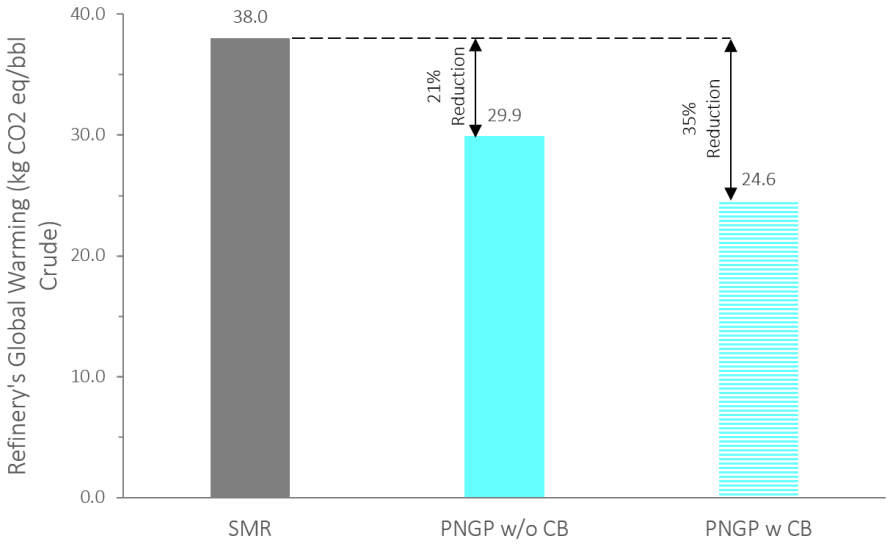


Figure 4.19: Typical petroleum refinery emissions with hydrogen from SMR versus PNGP

the refinery are about 38 kilograms of $CO_2$ equivalent per barrel of crude oil, with SMR contributing 10 kilograms. As depicted in Figure 4.19, transitioning the hydrogen production from SMR to PNGP presents a noteworthy 21% reduction in the total GHG emissions of the refinery when considering the scenario excluding carbon black production credits by PNGP. Incorporating these credits leads to an even more reduction of 35% in refinery emissions. These substantial emission reductions underscore the potential significance of such technology transitions in aiding Canada's oil and gas sector toward achieving its near-term emission reduction targets within the framework of Canada's 2030 emission reduction plan [9].

# Chapter 5

# Conclusion

Hydrogen plays a pivotal role in achieving global net-zero objectives, serving as a clean energy resource for various sectors, including transportation, heavy industries, and chemical production. However, the current state of hydrogen production heavily relies on fossil fuels, with natural gas, oil, and coal dominating the sources, resulting in substantial greenhouse gas emissions. There is a shift in the envisioned hydrogen production towards water electrolysis in the net-zero emission scenario of 2050. Nonetheless, current water electrolysis methods are energy-intensive, with significant electricity consumption, and are not entirely green due to the high reliance on fossil fuel-based electricity generation. As we strive towards net-zero goals, the environmental situation calls for short-term solutions to serve as a bridge between the present and a sustainable future for hydrogen production.

The evaluation of natural gas pyrolysis for hydrogen production, encompassing technical, economic, and environmental aspects, provides valuable insights into its potential as a viable alternative to conventional hydrogen production technologies.

From a technical perspective, plasma-assisted natural gas pyrolysis (PNGP) demonstrates impressive conversion efficiency, achieving almost complete decomposition of natural gas into carbon particles and hydrogen. This high conversion efficiency is a promising feature of PNGP, highlighting its potential to contribute to the efficient utilization of natural gas resources. However, it is important to note that PNGP requires a higher amount of energy compared to steam methane reforming (SMR). This higher energy requirement emphasizes the significance of selecting an appropriate

electricity source, preferably renewable energy, to mitigate the environmental impacts associated with electricity generation.

Economically, the minimum selling price (MSP) analysis reveals the cost competitiveness of PNGP compared to SMR, SMR with carbon capture and storage (CCS), and PEM electrolysis. The results indicate that PNGP, without considering the revenue generated from carbon black production, falls short in terms of cost-effectiveness when compared to SMR. However, incorporating carbon black production credits significantly improves PNGP's economic performance, making it competitive with SMR with CCS. This highlights the importance of considering the potential revenue streams from valuable byproducts in evaluating the overall economic viability of hydrogen production processes.

In terms of environmental impacts assessment, the results indicate that PNGP exhibits higher impacts in certain categories such as water consumption, ozone formation, and land use compared to SMR and SMR with CCS, regardless of the inclusion of carbon black production credits. However, PNGP demonstrates better performance in categories related to human health and ecosystem quality, especially when renewable electricity sources are employed. These findings underscore the need to carefully consider the trade-offs between different environmental impact categories when assessing the sustainability of hydrogen production technologies.

Upon comparing the cost of avoided/captured greenhouse gas (GHG) emissions between PNGP and SMR with CCS, it is evident that PNGP demonstrates competitive results when carbon black production credits are considered. At specific electricity and natural gas price levels, the costs of avoided/captured emissions favor PNGP over SMR with CCS. However, it is essential to note that while SMR with CCS may yield better results in certain scenarios, such as when carbon black production credits are not included in the calculations, it has limitations related to the availability of suitable formations for carbon dioxide storage. This restricts the applicability of SMR with CCS in certain cases. Hence, considering both technical and environmental aspects, PNGP shows promise as a potential low-emission hydrogen production method, especially when accounting for the added value of carbon black production.

In conclusion, while plasma-assisted natural gas pyrolysis demonstrates technical efficiency, the

economic competitiveness and environmental performance of the process need to be further optimized and enhanced. Continued research and development efforts, along with advancements in renewable energy integration, process optimization, and carbon byproduct utilization, hold the potential to position PNGP as a sustainable and economically viable solution for hydrogen production, contributing to a greener and more sustainable energy future.

## 5.1 Future Works

Our future research endeavors will center on the integration of plasma-assisted natural gas pyrolysis with emerging carbon dioxide hydrogenation technologies, aimed at converting $CO_2$ into valuable products instead of mere storage in deep formations. These pathways will undergo thorough investigation, encompassing assessments of their economic performance and environmental impacts. By conducting comprehensive studies in this regard, we aim to gain deeper insights into the feasibility, advantages, and potential challenges associated with these carbon dioxide utilization routes. Such investigations hold the potential to contribute substantially to the knowledge and viability of harnessing carbon dioxide for valuable purposes while fostering sustainable and environmentally responsible hydrogen production practices.

# Appendix A

## A.1 Purchased Equipment Costs and Process Flow Diagram

Table A.1: Purchased equipment costs for $100 tonnes/day$ hydrogen production capacity

| Equipment | Cost (USD) | Reference |
|---|---|---|
| NG Pyrolysis Section | | |
| Plasma Reactor | 36,127,080 | [47] |
| Hydrogen PSA | 2,782,003 | [62] |
| Plasma Preheater | 349,608 | APEA |
| Feed Preheater 1 | 165,042 | APEA |
| Feed Preheater 2 | 233,072 | APEA |
| Heat Exchanger 1 | 37,523 | APEA |
| Heat Exchanger 2 | 153,449 | APEA |
| Heat Exchanger 3 | 114,401 | APEA |
| Gas/Solid Filter | 292,561 | APEA |
| Recycled H2 Compressor | 2,435,055 | APEA |
| H2 Product Compressor | 5,361,881 | APEA |
| Recycled HC Compressor | 1,887,763 | APEA |
| Turboexpander | 577,494 | APEA |
| Carbon Black Processing Section | | |
| Carbon Black Granulator | 903,519 | APEA |
| Carbon Black Dryer | 374319 | APEA |
| Air Blower | 74,742 | APEA |
| Heat Exchanger 4 | 31,727 | APEA |
| Pump 1 | 75,352 | APEA |
| Power Generation Section | | |
| Waste Heat Boiler | 725,147 | APEA |
| Steam Turbine | 600,069 | APEA |
| Electrical Generator | 2,028,399 | APEA |
| Heat Exchanger 5 | 179,990 | APEA |
| Pump 2 | 76,267 | APEA |

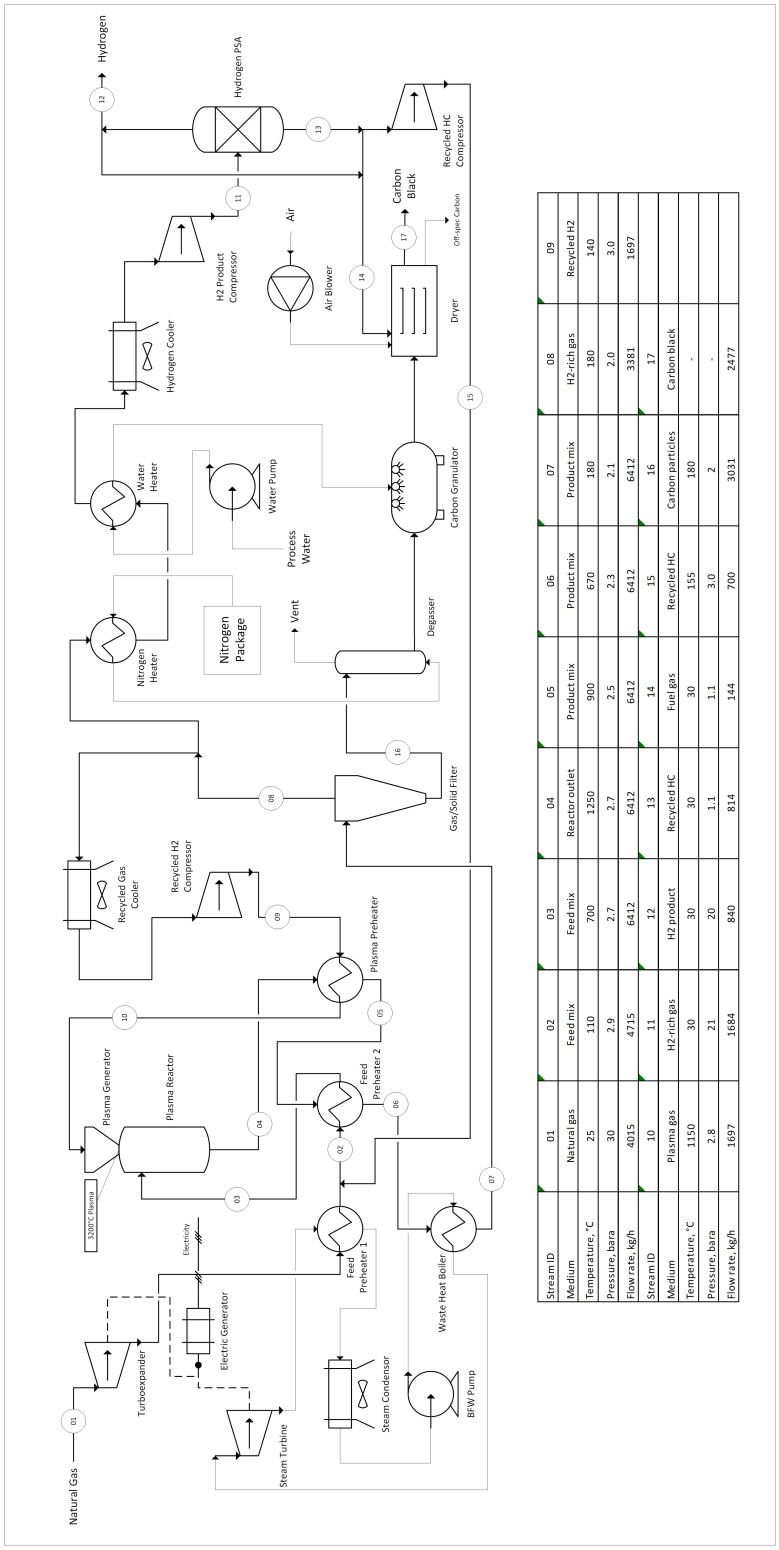


| Stream ID | 01 | 02 | 03 | 04 | 05 | 06 | 07 | 08 | 09 |
|---|---|---|---|---|---|---|---|---|---|
| Medium | Natural gas | Feed mix | Feed mix | Reactor outlet | Product mix | Product mix | Product mix | H2-rich gas | Recycled H2 |
| Temperature, °C | 25 | 110 | 700 | 1250 | 900 | 670 | 180 | 180 | 140 |
| Pressure, bara | 30 | 2.9 | 2.7 | 2.7 | 2.5 | 2.3 | 2.1 | 2.0 | 3.0 |
| Flow rate, kg/h | 4015 | 4715 | 6412 | 6412 | 6412 | 6412 | 6412 | 3381 | 1697 |
| Stream ID | 10 | 11 | 12 | 13 | 14 | 15 | 16 | 17 | |
| Medium | Plasma gas | H2-rich gas | H2 product | Recycled HC | Fuel gas | Recycled HC | Carbon particles | Carbon black | |
| Temperature, °C | 1150 | 30 | 30 | 30 | 30 | 155 | 180 | - | |
| Pressure, bara | 2.8 | 21 | 20 | 1.1 | 1.1 | 3.0 | 2 | - | |
| Flow rate, kg/h | 1697 | 1684 | 840 | 814 | 144 | 700 | 3031 | 2477 | |

Figure A.1: NG Pyrolysis Flow Diagram

## A.2 ReCiPe Midpoint Result Details

Figures A.2, A.3, and A.4 provide comprehensive insights into the toxicity and ozone formation impacts under six distinct electricity generation scenarios. Additionally, Figures A.5, A.6, and A.7 present detailed results concerning the midpoint impacts of various hydrogen production methods in BC, Canada.

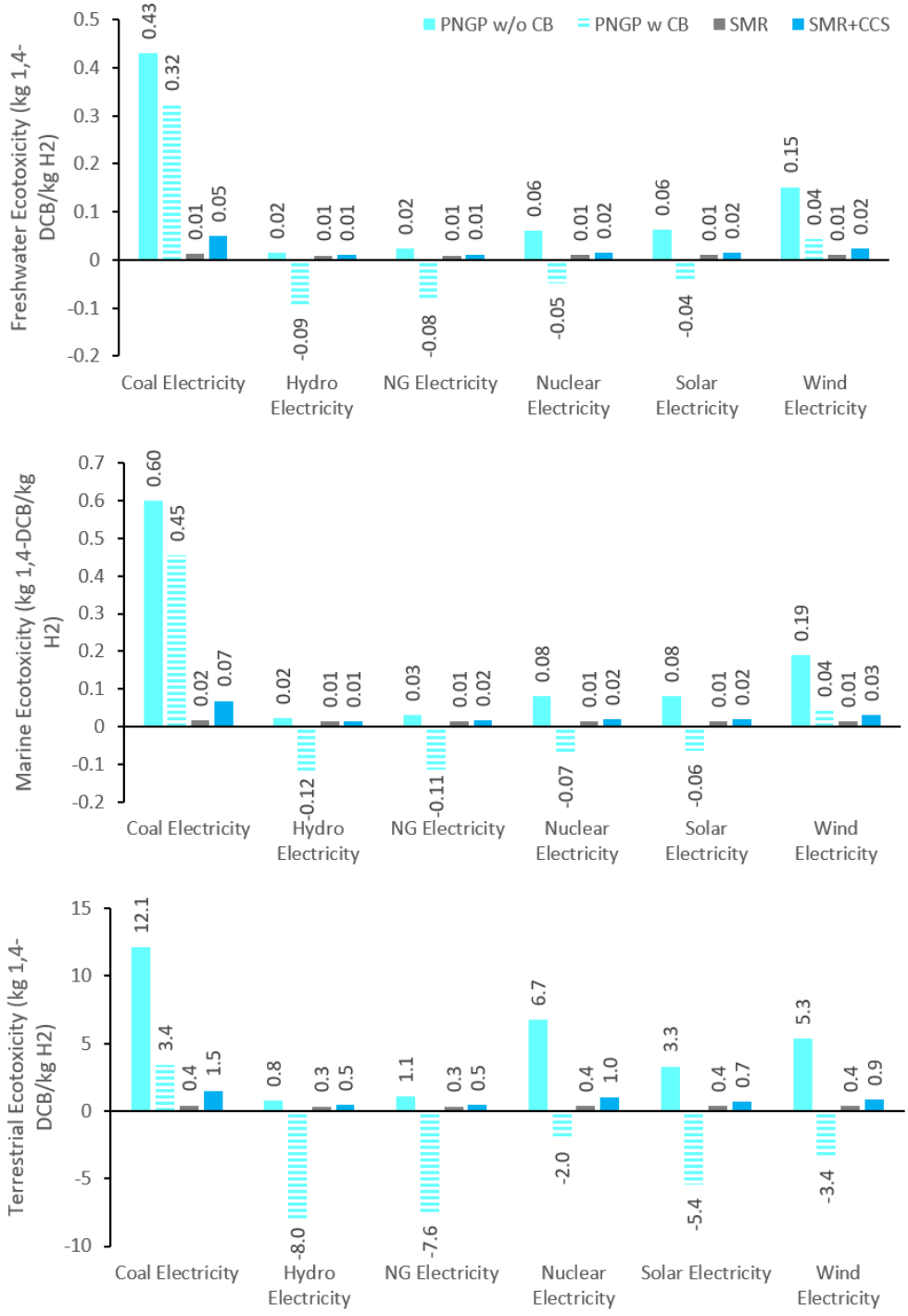


Figure A.2: ReCiPe midpoint toxicity results under different electricity scenarios - part 1

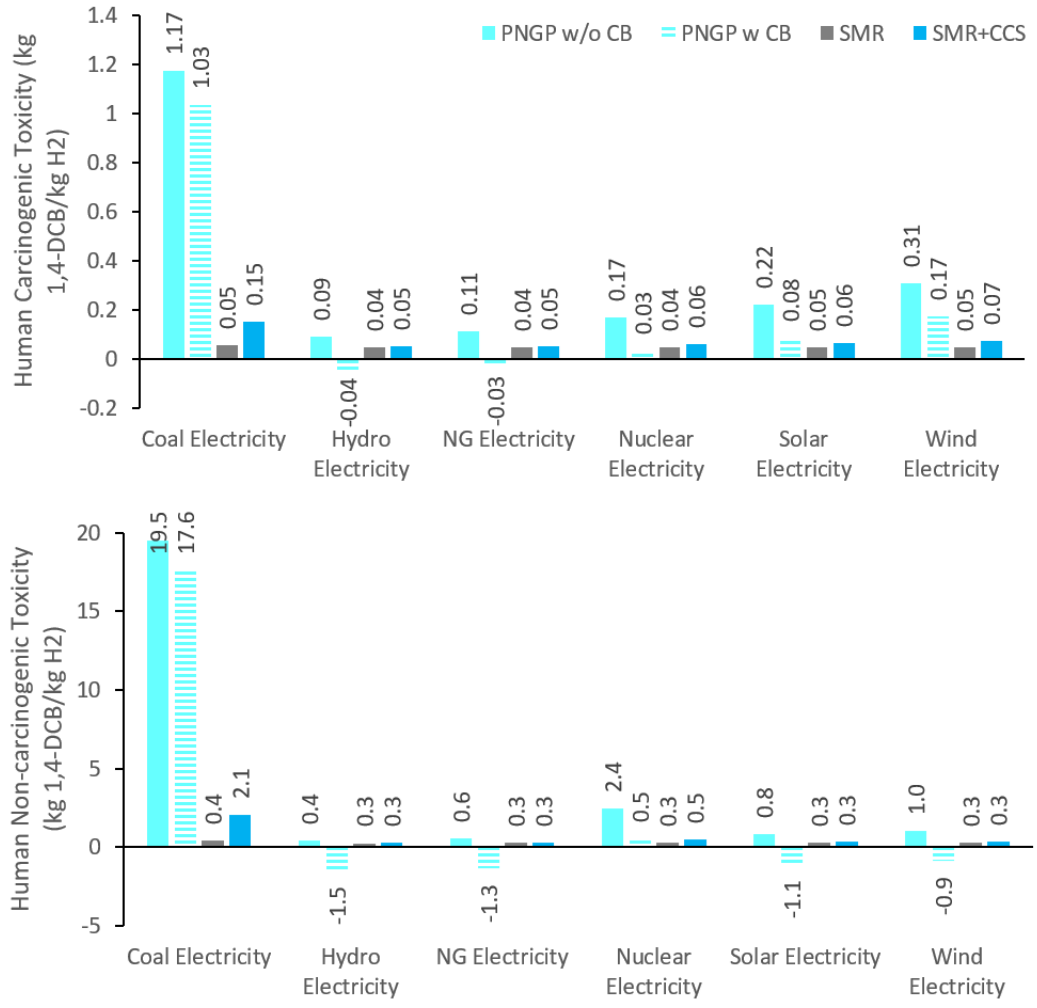


Figure A.3: ReCiPe midpoint toxicity results under different electricity scenarios - part 2

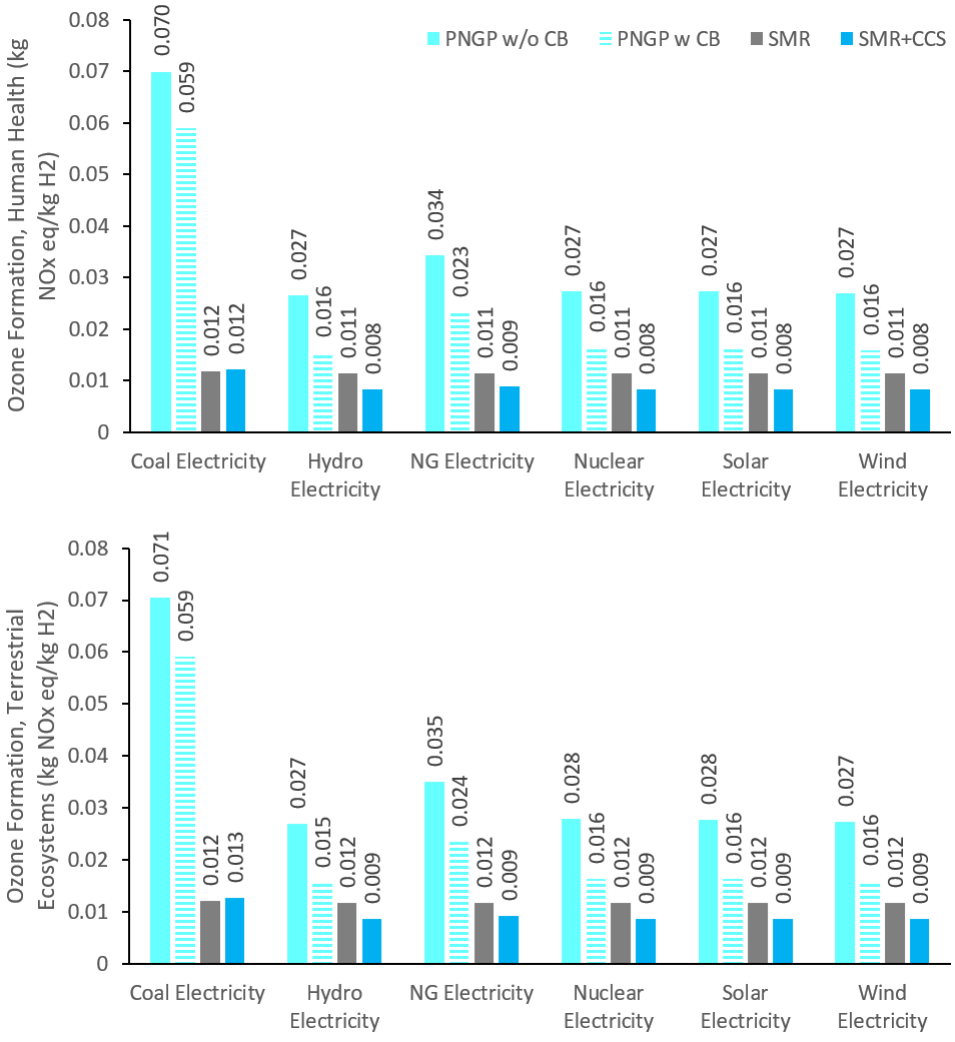


Figure A.4: ReCiPe midpoint ozone formation results under different electricity scenarios

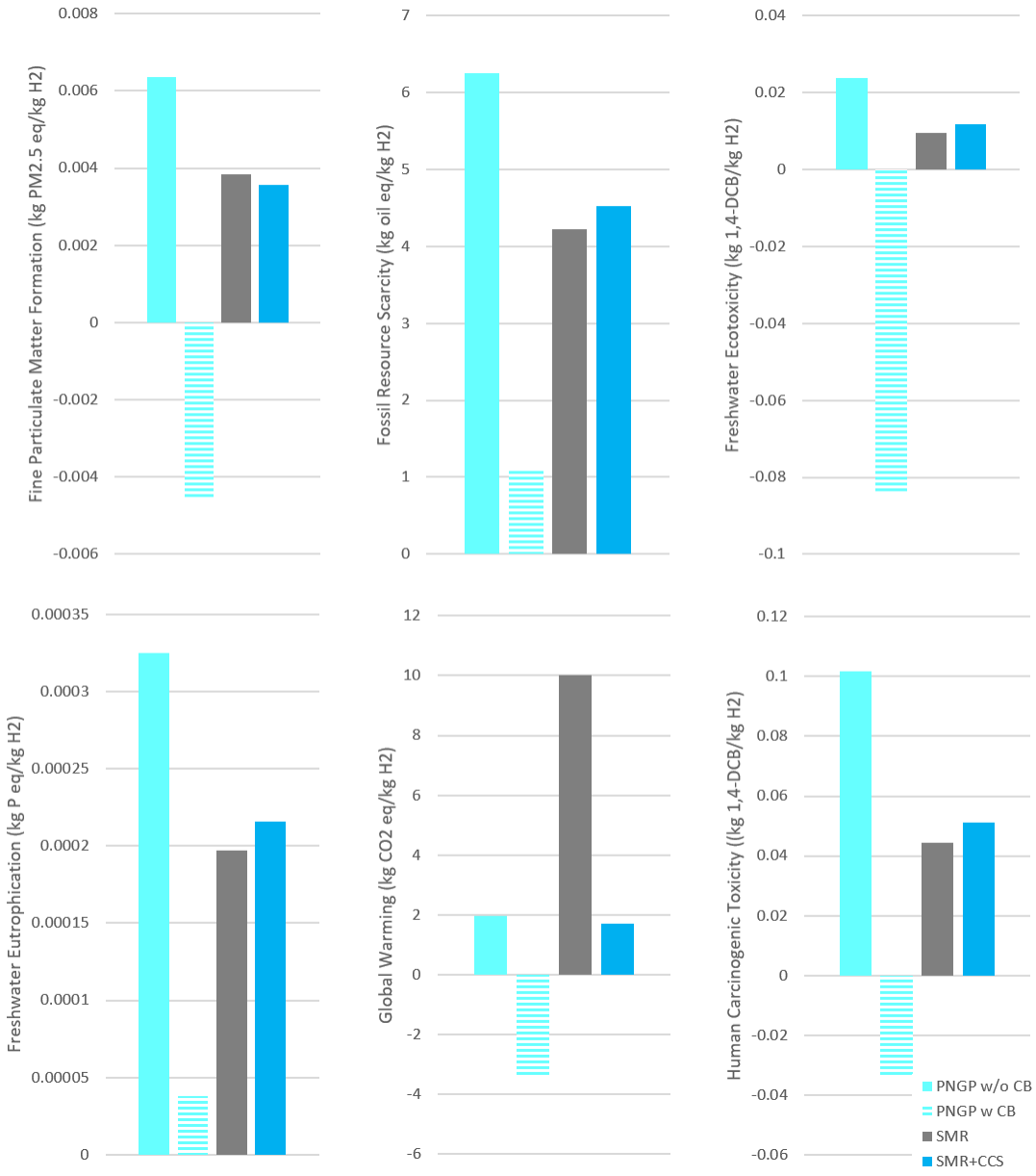


Figure A.5: ReCiPe midpoint results of different hydrogen production methods in BC, Canada - part 1

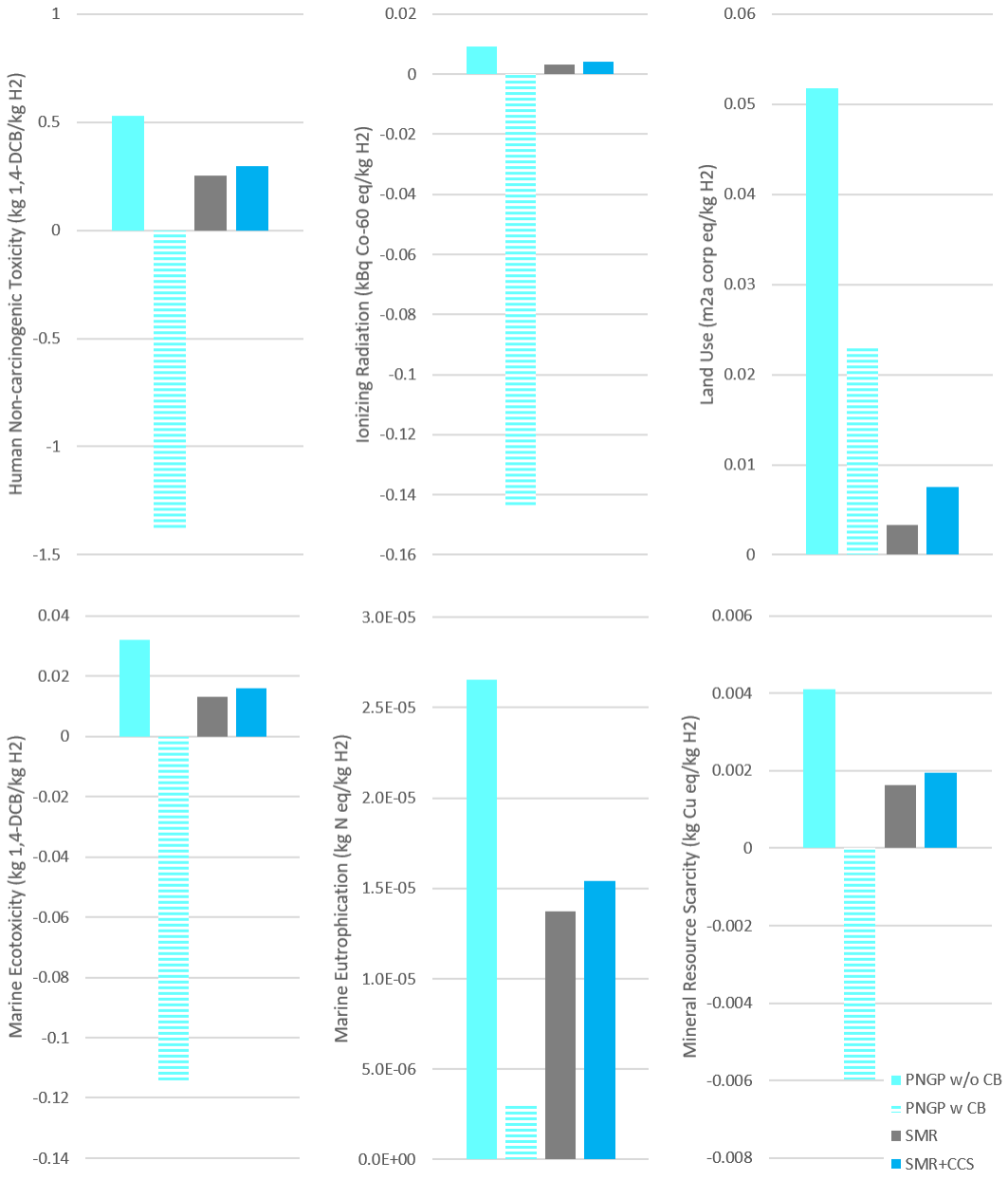


Figure A.6: ReCiPe midpoint results of different hydrogen production methods in BC, Canada - part 2

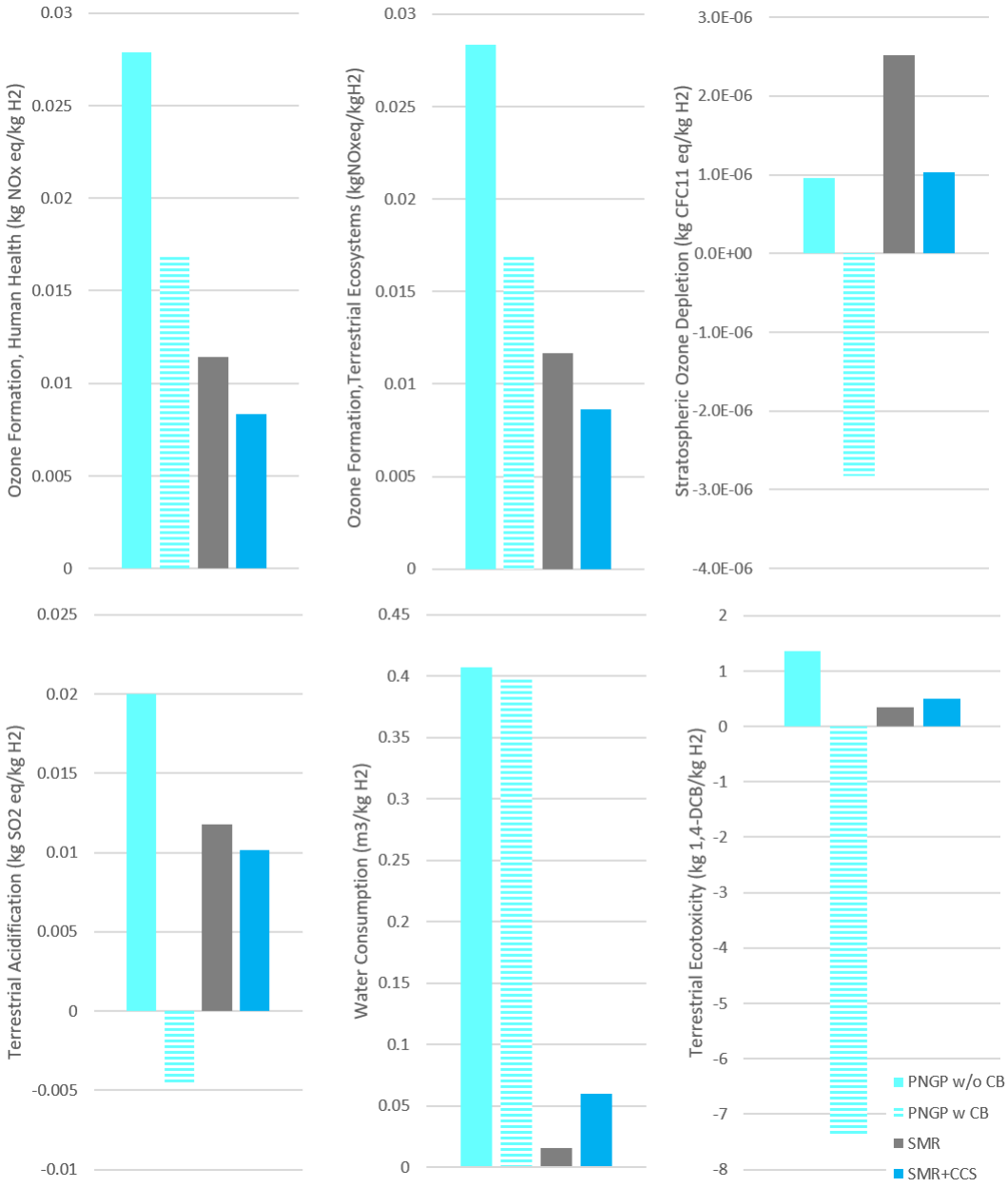


Figure A.7: ReCiPe midpoint results of different hydrogen production methods in BC, Canada - part 3

# Bibliography


[1] R. Kothari, D. Buddhi, and R. Sawhney, "Comparison of environmental and economic aspects of various hydrogen production methods," *Renewable and Sustainable Energy Reviews*, vol. 12, no. 2, pp. 553–563, 2008. [Online]. Available: https://www.sciencedirect.com/science/article/pii/S1364032106001158

[2] I. (2022), "Hydrogen," IEA, Paris. https://www.iea.org/reports/hydrogen, License: CC BY 4.0, Tech. Rep.

[3] P. L. Spath and M. K. Mann, "Life cycle assessment of hydrogen production via natural gas steam reforming." [Online]. Available: https://www.osti.gov/biblio/764485

[4] I. (2021), "Net Zero by 2050, Paris https://www.iea.org/reports/net-zero-by-2050, License: CC BY 4.0," Tech. Rep.

[5] S. Grigoriev, V. Fateev, D. Bessarabov, and P. Millet, "Current status, research trends, and challenges in water electrolysis science and technology," *International Journal of Hydrogen Energy*, vol. 45, no. 49, pp. 26 036–26 058, 2020, progress in Hydrogen Production and Utilization. [Online]. Available: https://www.sciencedirect.com/science/article/pii/S0360319920310715

[6] N. Muradov, "Low to near-zero co2 production of hydrogen from fossil fuels: Status and perspectives," *International Journal of Hydrogen Energy*, vol. 42, no. 20, pp. 14 058–14 088, 2017. [Online]. Available: https://www.sciencedirect.com/science/article/pii/S0360319917314908

[7] R. A. Dagle, V. Dagle, M. D. Bearden, J. D. Holladay, T. R. Krause, and S. Ahmed, "An overview of natural gas conversion technologies for co-production of hydrogen and value-added solid carbon products." [Online]. Available: https://www.osti.gov/biblio/1411934

[8] S. Timmerberg, M. Kaltschmitt, and M. Finkbeiner, "Hydrogen and hydrogen-derived fuels through methane decomposition of natural gas – ghg emissions and costs," *Energy Conversion and Management: X*, vol. 7, p. 100043, 2020. [Online]. Available: https://www.sciencedirect.com/science/article/pii/S2590174520300155

[9] *2030 emissions reduction plan: Canada's next steps to clean air and a strong economy*. Gatineau, QC: Environment and Climate Change Canada = Environnement et changement climatique Canada, 2022, oCLC: 1317803653.

[10] IRENA, "Geopolitics of the Energy Transformation: The Hydrogen Factor," International Renewable Energy Agency, Abu Dhabi, Tech. Rep., 2022. [Online]. Available: www.irena.org/publications

[11] M. Younas, S. Shafique, A. Hafeez, F. Javed, and F. Rehman, "An overview of hydrogen production: Current status, potential, and challenges," *Fuel*, vol. 316, p. 123317, 2022. [Online]. Available: https://www.sciencedirect.com/science/article/pii/S0016236122001867

[12] Y. K. Salkuyeh, B. A. Saville, and H. L. MacLean, "Techno-economic analysis and life cycle assessment of hydrogen production from natural gas using current and emerging technologies," *International Journal of Hydrogen Energy*, vol. 42, no. 30, pp. 18 894–18 909, 2017. [Online]. Available: https://www.sciencedirect.com/science/article/pii/S0360319917322036

[13] I. (2022), "Global Hydrogen Review 2022, IEA, Paris https://www.iea.org/reports/global-hydrogen-review-2022, License: CC BY 4.0," Tech. Rep.

[14] A. Buttler and H. Spliethoff, "Current status of water electrolysis for energy storage, grid balancing and sector coupling via power-to-gas and power-to-liquids: A review," *Renewable and Sustainable Energy Reviews*, vol. 82, pp. 2440–2454, 2018. [Online]. Available: https://www.sciencedirect.com/science/article/pii/S136403211731242X

[15] "EIA International Energy Statistics database," U.S. Energy Information Administration, Tech. Rep. [Online]. Available: www.eia.gov/international/data/world

[16] B. Lee, H.-S. Cho, H. Kim, D. Lim, W. Cho, C.-H. Kim, and H. Lim, "Integrative techno-economic and environmental assessment for green H2 production by alkaline water electrolysis based on experimental data," *Journal of Environmental Chemical Engineering*, vol. 9, no. 6, p. 106349, 2021. [Online]. Available: https://www.sciencedirect.com/science/article/pii/S2213343721013269

[17] G. Palmer, A. Roberts, A. Hoadley, R. Dargaville, and D. Honnery, "Life-cycle greenhouse gas emissions and net energy assessment of large-scale hydrogen production via electrolysis and solar PV," *Energy Environ. Sci.*, vol. 14, no. 10, pp. 5113–5131, 2021, publisher: The Royal Society of Chemistry. [Online]. Available: http://dx.doi.org/10.1039/D1EE01288F

[18] H. F. Abbas and W. M. A. W. Daud, "Hydrogen production by methane decomposition: A review," *International Journal of Hydrogen Energy*, vol. 35, no. 3, pp. 1160–1190, 2010. [Online]. Available: https://www.sciencedirect.com/science/article/pii/S0360319909018059

[19] J. Li and K. J. Smith, "Methane decomposition and catalyst regeneration in a cyclic mode over supported Co and Ni catalysts," *Applied Catalysis A: General*, vol. 349, no. 1, pp. 116–124, 2008. [Online]. Available: https://www.sciencedirect.com/science/article/pii/S0926860X08004432

[20] M. S. Rahman, E. Croiset, and R. R. Hudgins, "Catalytic Decomposition of Methane for Hydrogen Production," *Topics in Catalysis*, vol. 37, no. 2-4, pp. 137–145, Apr. 2006. [Online]. Available: http://link.springer.com/10.1007/s11244-006-0015-8

[21] H. T. Jang and W. S. Cha, "Hydrogen production by the thermocatalytic decomposition of methane in a fluidized bed reactor," *Korean Journal of Chemical Engineering*, vol. 24, no. 2, pp. 374–377, Mar. 2007. [Online]. Available: http://link.springer.com/10.1007/s11814-007-5037-9

[22] K. Otsuka, S. Takenaka, and H. Ohtsuki, "Production of pure hydrogen by cyclic

decomposition of methane and oxidative elimination of carbon nanofibers on supported-Ni-based catalysts," *Applied Catalysis A: General*, vol. 273, no. 1, pp. 113–124, 2004. [Online]. Available: https://www.sciencedirect.com/science/article/pii/S0926860X04005800

[23] N. Muradov, F. Smith, and A. T-Raissi, "Catalytic activity of carbons for methane decomposition reaction," *Catalysis Today*, vol. 102-103, pp. 225–233, May 2005. [Online]. Available: https://linkinghub.elsevier.com/retrieve/pii/S0920586105000301

[24] M. Kim, "Hydrogen production by catalytic decomposition of methane over activated carbons: kinetic study," *International Journal of Hydrogen Energy*, vol. 29, no. 2, pp. 187–193, Feb. 2004. [Online]. Available: https://linkinghub.elsevier.com/retrieve/pii/S0360319903001113

[25] N. Muradov, Z. Chen, and F. Smith, "Fossil hydrogen with reduced emission: Modeling thermocatalytic decomposition of methane in a fluidized bed of carbon particles," *International Journal of Hydrogen Energy*, vol. 30, no. 10, pp. 1149–1158, Aug. 2005. [Online]. Available: https://linkinghub.elsevier.com/retrieve/pii/S036031990500090X

[26] R. Aiello, J. E. Fiscus, H.-C. z. Loye, and M. D. Amiridis, "Hydrogen production via the direct cracking of methane over Ni/SiO2: catalyst deactivation and regeneration," *Applied Catalysis A: General*, vol. 192, no. 2, pp. 227–234, 2000. [Online]. Available: https://www.sciencedirect.com/science/article/pii/S0926860X99003452

[27] H. F. Abbas and W. M. A. W. Daud, "Thermocatalytic decomposition of methane for hydrogen production using activated carbon catalyst: Regeneration and characterization studies," *International Journal of Hydrogen Energy*, vol. 34, no. 19, pp. 8034–8045, 2009. [Online]. Available: https://www.sciencedirect.com/science/article/pii/S0360319909012634

[28] S. Schneider, S. Bajohr, F. Graf, and T. Kolb, "State of the art of hydrogen production via pyrolysis of natural gas," *ChemBioEng Reviews*, vol. 7, no. 5, pp. 150–158, 2020. [Online]. Available: https://onlinelibrary.wiley.com/doi/abs/10.1002/cben.202000014

[29] D. Lee, "Hydrogen production via the Kværner process and plasma reforming," in *Compendium of Hydrogen Energy*. Elsevier, 2015, pp. 349–391. [Online]. Available: https://linkinghub.elsevier.com/retrieve/pii/B9781782423614000121

[30] N. J. Hardman, R. W. Taylor, A. F. Hoermann, P. L. Johnson, C. J. Cardinal, and R. J. Hanson, "Carbon Black From Natural Gas," United Stated Patent US10 808 097B2, Oct., 2020. [Online]. Available: https://patents.google.com/patent/US10808097B2/en

[31] J. A. Bakken, R. Jensen, B. Monsen, O. Raaness, and A. N. Wærnes, "Thermal plasma process development in norway," *Pure and Applied Chemistry*, vol. 70, no. 6, pp. 1223–1228, 1998. [Online]. Available: https://doi.org/10.1351/pac199870061223

[32] M. Gautier, V. Rohani, and L. Fulcheri, "Direct decarbonization of methane by thermal plasma for the production of hydrogen and high value-added carbon black," *International Journal of Hydrogen Energy*, vol. 42, no. 47, pp. 28 140–28 156, Nov. 2017. [Online]. Available: https://www.sciencedirect.com/science/article/pii/S0360319917336492

[33] L. Fulcheri and Y. Schwob, "From methane to hydrogen, carbon black and water," *International Journal of Hydrogen Energy*, vol. 20, no. 3, pp. 197–202, 1995. [Online]. Available: https://www.sciencedirect.com/science/article/pii/0360319994E0022Q

[34] J. R. Fincke, R. P. Anderson, T. A. Hyde, and B. A. Detering, "Plasma pyrolysis of methane to hydrogen and carbon black," *Industrial & Engineering Chemistry Research*, vol. 41, no. 6, pp. 1425–1435, 2002. [Online]. Available: https://doi.org/10.1021/ie010722e

[35] A. R. d. C. Labanca, "Carbon black and hydrogen production process analysis," *International Journal of Hydrogen Energy*, vol. 45, no. 47, pp. 25 698–25 707, 2020. [Online]. Available: https://www.sciencedirect.com/science/article/pii/S0360319920310181

[36] N. J. Hardman, R. W. Taylor, R. J. Hanson, and P. L. Johnson, "Carbon Black Generating System," U.S. Patent US2018/0 022 925A1, Jan., 2018. [Online]. Available: https://patents.google.com/patent/US20180022925

[37] A. F. Hoermann, P. L. Johnson, N. S. Myklebust, and M. M. Nordvik, "Plasma Torch Design," U.S. Patent US2015/0 223 314A1, Aug., 2015. [Online]. Available: https://patents.google.com/patent/US20150223314

[38] P. L. Johnson, R. J. Hanson, and R. W. Taylor, "Plasma Reactor," U.S. Patent WO2015/116 811A1, Aug., 2015. [Online]. Available: https://patents.google.com/patent/WO2015116811A1/en

[39] R. W. Taylor and A. F. Hoermann, "Regenerative Cooling Method and Apparstus," U.S. Patent US10 618 026B2, Apr., 2020. [Online]. Available: https://patents.google.com/patent/US10618026B2/en

[40] R. W. Taylor, A. F. Hoermann, P. L. Johnson, and A. S. Hampton, "Secondary Heat Addition to Particle Production Process and Apparatus," U.S. Patent US2019/0 100 658, Apr., 2019. [Online]. Available: https://patents.google.com/patent/US20190100658A1/en

[41] ChemAnalyst, "Carbon Black Market Analysis: Industry Market Size, Plant Capacity, Process, Operating Efficiency, Demand & Supply, End-Use, Foreign Trade, Grade, Type, Sales Channel, Regional Demand, Company Share, 2015-2035," May 2023. [Online]. Available: https://www.chemanalyst.com/industry-report/carbon-black-market-440

[42] "Construction Permit Application for Monolith Nebraska, LLC Olive Greek 2 (OG2)," EA Engineering, Science, and Technology Inc., Tech. Rep., Mar. 2021. [Online]. Available: https://api.oilandgaswatch.org/d/94/d7/94d75b345dce431a9dc864463c80e272.1640126219.pdf

[43] A. F. Hoermann, R. W. Taylor, and N. S. Myklebust, "Plasma Gas Throat Assembly and Method," US Patent WO/2015/116 800, Jul., 2015. [Online]. Available: https://patents.google.com/patent/WO2015116800A1/en

[44] G. Kozlov and V. Knorre, "Single-pulse shock tube studies on the kinetics of the thermal decomposition of methane," *Combustion and Flame*, vol. 6, pp. 253–263, Jan. 1962. [Online]. Available: https://www.sciencedirect.com/science/article/pii/0010218062901037

[45] P. L. Johnson and R. W. Taylor, "High Temperature Heat Integration Method of Making Carbon Black," U.S. Patent US2017/0 058 128A1, Mar., 2017. [Online]. Available: https://patents.google.com/patent/US20170058128A1/en?assignee=Monolith+Materials%2c+Inc.&page=2

[46] R. W. Taylor and P. L. Johnson, "Carbon Black Combustible Gas Separation," U.S. Patent US2018/0 016 441A1, Jan., 2018. [Online]. Available: https://patents.google.com/patent/US20180016441A1/en?assignee=Monolith+Materials%2c+Inc.&page=1

[47] H. A. Gabbar, S. A. Darda, V. Damideh, I. Hassen, M. Aboughaly, and D. Lisi, "Comparative study of atmospheric pressure DC, RF, and microwave thermal plasma torches for waste to energy applications," *Sustainable Energy Technologies and Assessments*, vol. 47, p. 101447, Oct. 2021. [Online]. Available: https://linkinghub.elsevier.com/retrieve/pii/S2213138821004574

[48] S. Sircar and T. C. Golden, "Purification of Hydrogen by Pressure Swing Adsorption," *Separation Science and Technology*, vol. 35, no. 5, pp. 667–687, Jan. 2000. [Online]. Available: http://www.tandfonline.com/doi/abs/10.1081/SS-100100183

[49] T. Skills, "Cost Indices," 2023. [Online]. Available: https://toweringskills.com/financial-analysis/cost-indices/

[50] U. B. of Labour Statistics, "Occupational Employment and Wage Statistics," 2021. [Online]. Available: https://www.bls.gov/oes/current/oes518091.htm#nat

[51] R. Smith, *Chemical Process Design and Integration*, 1st ed. John Wiley & Sons, Ltd, 2005.

[52] M. S. Peters, K. D. Timmerhaus, and R. E. West, *Plant Design and Economics for Chemical Engineers, Fifth Edition*, 5th ed. McGraw-Hill, 2003.

[53] D. W. Green and M. Z. Southard, Eds., *Perry's chemical engineers' handbook*, ninth edition, 85th anniversary edition ed. New York: McGraw Hill Education, 2019, oCLC: on1019739383.

[54] W. D. Seider, J. D. Seader, and D. R. Lewin, *Product and Process Design Principles: Synthesis, Analysis, and Evaluation*, 2nd ed. John Wiley & Sons, Ltd, 2003.

[55] NREL, "H2A: Hydrogen Analysis Production Models." [Online]. Available: https://www.nrel.gov/hydrogen/h2a-production-models.html

[56] YCHARTS, "US Producer Price Index: Chemicals and Allied Products: Carbon Black (I:USPPE4BW)," May 2023. [Online]. Available: https://ycharts.com/indicators/us_producer_price_index_chemicals_and_allied_products_carbon_black

[57] Statista, "Average Industrial Electricity Prices in Canada as of April 2022, by Select City," Mar. 2023. [Online]. Available: https://www.statista.com/statistics/579159/average-industrial-electricity-prices-canada-by-major-city/

[58] eia, "Henry Hub Natural Gas Spot Price," 2023. [Online]. Available: https://www.eia.gov/dnav/ng/hist/rngwhhdA.htm

[59] M. Wang, A. Elgowainy, Z. Lu, K. H. Baek, A. Bafana, P. T. Benavides, A. Burnham, H. Cai, V. Cappello, P. Chen, Y. Gan, U. R. Gracida-Alvarez, T. R. Hawkins, R. K. Iyer, J. C. Kelly, T. Kim, S. Kumar, H. Kwon, K. Lee, U. Lee, X. Liu, F. Masum, C. Ng, L. Ou, K. Reddi, N. Siddique, P. Sun, P. Vyawahare, H. Xu, and G. Zaimes, "Greenhouse gases, regulated emissions, and energy use in technologies model ® (2022 .net)," [Computer Software] https://doi.org/10.11578/GREET-Net-2022/dc.20220908.2, oct 2022. [Online]. Available: https://doi.org/10.11578/GREET-Net-2022/dc.20220908.2

[60] C. E. Regulator, "Provincial and Territorial Energy Profiles - Canada," Mar. 2023. [Online]. Available: https://www.cer-rec.gc.ca/en/data-analysis/energy-markets/provincial-territorial-energy-profiles/provincial-territorial-energy-profiles-canada.html

[61] J. A. Bergerson, J. P. Abella, K. Motazedi, J. Guo, K. Cousart, and L. Jing, "PRELIM: The Petroleum Refinery Life Cycle Inventory Model," 2022. [Online]. Available: https://www.ucalgary.ca/energy-technology-assessment/open-source-models/prelim

[62] I. Burgers, L. Dehdari, P. Xiao, K. G. Li, E. Goetheer, and P. Webley, "Techno-economic analysis of PSA separation for hydrogen/natural gas mixtures at hydrogen refuelling stations," *International Journal of Hydrogen Energy*, vol. 47, no. 85, pp. 36 163–36 174, 2022. [Online]. Available: https://www.sciencedirect.com/science/article/pii/S0360319922037788